A Random-Finite-Set Approach to Bayesian SLAM

John Mullane, Ba-Ngu Vo, Martin D. Adams, and Ba-Tuong Vo

***Abstract*—This paper proposes an integrated Bayesian framework for feature-based simultaneous localization and map building (SLAM) in the general case of uncertain feature number and data association. By modeling the measurements and feature map as random finite sets (RFSs), a formulation of the feature-based SLAM problem is presented that jointly estimates the number and location of the features, as well as the vehicle trajectory. More concisely, the joint posterior distribution of the set-valued map and vehicle trajectory is propagated forward in time as measurements arrive, thereby incorporating both data association and feature management into a single recursion. Furthermore, the Bayes optimality of the proposed approach is established.**

A first-order solution, which is coined as the probability hypothesis density (PHD) SLAM filter, is derived, which jointly propagates the posterior PHD of the map and the posterior distribution of the vehicle trajectory. A Rao–Blackwellized (RB) implementation of the PHD–SLAM filter is proposed based on the Gaussian-mixture PHD filter (for the map) and a particle filter (for the vehicle trajectory). Simulated and experimental results demonstrate the merits of the proposed approach, particularly in situations of high clutter and data association ambiguity.

***Index Terms*—Bayesian simultaneous localization and mapping (SLAM), feature-based map, point process, probability hypothesis density (PHD), random finite set (RFS).**

NOMENCLATURE

k	Current time index.
M_k	Feature-map random vector.
$\hat{M}_k$	Estimate of M_k.
X_k	Vehicle-pose random vector at k.
$X_{0:k}$	Vehicle-trajectory random vector.
$\hat{X}_{0:k}$	Estimate of $X_{0:k}$.
$\mathcal{M}$	Feature-map RFS.
$\mathcal{M}_k$	Explored-map RFS up to k.
$\hat{\mathcal{M}}_k$	Estimate of $\mathcal{M}_k$.
$\mathcal{Z}_k$	RFS sensor measurement.
$\mathcal{Z}_{0:k}$	History of RFS measurements.
$\mathcal{D}_k$	Feature-measurement RFS.
$\mathcal{C}_k$	Clutter-measurement RFS.
$\mathcal{B}_k$	RFS of the new features.
$p_{k\|k}(\mathcal{M}_k, X_{0:k}\|\cdot)$	Conditional pdf of RFS–SLAM.
$p_{k\|k}(\mathcal{M}_k\|\cdot)$	Conditional pdf of $\mathcal{M}_k$.
$p_{k\|k-1}(\mathcal{M}_k\|\cdot)$	Predicted conditional pdf of $\mathcal{M}_k$.
$g_k(\mathcal{Z}_k\|\cdot)$	Conditional pdf of $\mathcal{Z}_k$.
$f_{\mathcal{M}}(\cdot\|\mathcal{M}_{k-1})$	Transition density of the map RFS.
$f_X(\cdot\|X_{k-1})$	Vehicle transition density.
$f_{\mathcal{D}}(\cdot)$	Density of the feature-measurement RFS.
$f_{\mathcal{C}}(\cdot)$	Density of the clutter-measurement RFS.
$f_{\mathcal{B}}(\cdot)$	Density of the new feature RFS.
$v_{k\|k}(m\|\cdot)$	PHD of the explored map RFS, i.e., $\mathcal{M}_k$.
$v_{k\|k-1}(m\|\cdot)$	PHD of the predicted map, i.e., $\mathcal{M}_{k\|k-1}$.
$c_k(z\|\cdot)$	PHD of $\mathcal{C}_k$.
$b_k(m\|\cdot)$	PHD of $\mathcal{B}_k$.
$\mathfrak{m}_k$	Number of features in $\mathcal{M}_k$.
$\hat{\mathfrak{m}}_k$	Estimated number of features in $\mathcal{M}_k$.
m^i	ith feature in $\mathcal{M}_k$.
$\mathfrak{z}_k$	Number of measurements in $\mathcal{Z}_k$.
z^i	ith measurement in $\mathcal{Z}_k$.
$g_k(z\|m)$	Likelihood of z given feature m.
$P_D(m)$	Detection probability of feature m.
N	Number of particles.
$X_{0:k}^{(i)}$	ith sample trajectory.
$w_k^{(i)}$	Weight of ith sample trajectory.
$v_k^{(i)}(m\|X_{0:k}^{(i)})$	ith trajectory-conditioned PHD of $\mathcal{M}_k$.
$J_k^{(i)}$	Number of Gaussian components in the ith trajectory-conditioned PHD of $\mathcal{M}_k$.
$\eta_k^{(i,j)}$	Weight of the jth Gaussian component of the ith trajectory-conditioned PHD of $\mathcal{M}_k$.
$\mu_k^{(i,j)}$	Mean of the jth Gaussian component of the ith trajectory-conditioned PHD of $\mathcal{M}_k$.
$P_k^{(i,j)}$	Covariance of the jth Gaussian component of the ith trajectory-conditioned PHD of $\mathcal{M}_k$.
$\bar{d}^{(c)}(\hat{\mathcal{M}}_k, \mathcal{M}_k)$	Error between $\hat{\mathcal{M}}_k$ and $\mathcal{M}_k$, with cutoff parameter c.

Manuscript received February 4, 2010; revised May 14, 2010 and October 17, 2010; accepted December 14, 2010. Date of publication February 7, 2011; date of current version April 7, 2011. This paper was recommended for publication by Associate Editor C. Stachniss and Editor G. Oriolo upon evaluation of the reviewers' comments. This work was supported in part by the Singapore National Research Foundation through the Singapore–Massachusetts Institute of Technology Alliance for Research and Technology Center for Environmental Sensing and Modeling. The work of B.-N. Vo was supported in part by the Australian Research Council under Discovery Grant DP0880553. The work of B.-T. Vo was supported by the Australian Research Council under Discovery Grant DP0989007. This work was presented in part at the IEEE International Conference on Robotics and Automation, Anchorage, AK, May 3–8, 2010.

J. Mullane is with the School of Electrical and Electronic Engineering, Nanyang Technological University, 639798 Singapore (e-mail: jsmullane@ntu.edu.sg).

B.-N. Vo and B.-T. Vo are with the School of Electrical, Electronic and Computer Engineering, University of Western Australia, Crawley, W.A. 6009, Australia (e-mail: ba-ngu.vo@uwa.edu.au; ba-tuong.vo@uwa.edu.au).

M. D. Adams is with the Department of Electrical Engineering, University of Chile, Santiago 837-0451, Chile (e-mail: martin@ing.uchile.cl).

Digital Object Identifier 10.1109/TRO.2010.2101370

I. INTRODUCTION

FOLLOWING seminal developments in autonomous robotics [1], the problem of simultaneous localization and mapping (SLAM) gained widespread interest, with numerous

1552-3098/$26.00 © 2011 IEEE

potential applications ranging from robotic planetary exploration to intelligent surveillance. This paper focusses on the feature-based approach that decomposes physical environmental landmarks into parametric representations such as points, lines, circles, corners, etc., which are known as features. Feature-based maps are comprised of an unknown number of features at unknown spatial locations [2] and are widely used in the SLAM literature [3]– [7]. Estimating a feature map thus requires the joint estimation of the *number* and location of the features that have been covered by the sensor's field-of-view (FoV).

In the Bayesian paradigm, the feature-based SLAM problem (henceforth referred to as SLAM for compactness) amounts to jointly propagating the posterior distribution of the map and vehicle trajectory. Current state-of-the-art SLAM solutions comprise two separate steps [6]:

1) Determine the measurement (to feature) associations.
2) Given the associations, estimate the feature locations and vehicle pose via stochastic filtering.

This two-tiered approach is efficient and works well for a wide range of applications [4], [6], [7] but is sensitive to data association (DA) uncertainty [8]. A SLAM solution that is robust to DA uncertainty under high clutter and measurement noise requires a framework that fully integrates DA uncertainty into the estimation of the map (and vehicle trajectory).

This paper advocates a fully integrated Bayesian framework for SLAM under DA uncertainty and unknown feature number. The key to this formulation is the representation of the map as a *finite set* of features. Indeed, from an estimation viewpoint, it is argued in Section II-A that the map should be represented by a finite set. Using random-finite-set (RFS) theory, SLAM is then posed as a Bayesian filtering problem in which the joint posterior distribution of the vehicle trajectory and set-valued map are propagated forward in time as measurements arrive. This so-called RFS–SLAM framework allows for the joint recursive estimation of the vehicle trajectory, the feature locations, and the number of features in the map. Moreover, it is shown that the proposed RFS approach is Bayes optimal.

The RFS formulation for SLAM was first proposed in [9], with preliminary studies using "brute force" implementations also appearing in [10]. The approach modeled the joint vehicle trajectory and map as a single RFS and recursively propagates its first-order moment. In this paper, however, a tractable first-order approximation, which is coined as the probability hypothesis density (PHD)–SLAM filter, is derived, which first factorizes the RFS–SLAM density and then propagates the posterior PHDs of multiple trajectory-conditioned maps and the posterior distribution of the vehicle trajectory. The PHD is the first-order moment of the RFS of the map and is closely related to the occupancy grid representation, as discussed later in Section IV-B. Furthermore, as presented in this paper, the RFS approach to SLAM admits the concept of an "expected" map via the PHD construct, which is not available in existing SLAM approaches.

This factorized approach to SLAM was established in the, now well known, FastSLAM concept [6]. However, it will be shown that the same factorization method applied to vectors in FastSLAM cannot be applied to sets, since it results in invalid densities in the feature space. Therefore, one of the main contributions of this paper is a technique that allows such a factorization to be applied to sets in a principled manner. Preliminary results have been announced in [6], and this paper presents a more rigorous analysis of the RFS approach to SLAM, an improved version of the PHD–SLAM filter, a discussion of Bayes optimality, as well as simulated and real experimental results. The merits of the RFS approach are demonstrated, particularly in situations of high clutter and DA ambiguity.

The paper is organized as follows. Section II demonstrates that the feature map can be represented as a finite set of features and proposes a corresponding Bayesian filtering framework for SLAM. Given the joint posterior density of the random-vector-vehicle trajectory and RFS feature map, optimal estimators are introduced and discussed in Section III. The PHD–SLAM filter, which propagates the first-order-moment of the RFS map, is presented in Section IV. Section V outlines a Rao–Blackwellized (RB) implementation of the PHD–SLAM filter, with Section VI presenting and discussing its performance. Extensions of the approach to incorporate other useful RFS representations are also presented.

II. Bayesian Random Finite-Set (Feature-Based) Simultaneous Localization and Mapping

This section discusses the mathematical representation of the map and presents a Bayesian formulation of the SLAM problem subject to uncertainty in DA and the number of features. In particular, it is argued that fundamentally, the map should be represented as a finite set, and thus, the concept of an RFS is required for a Bayesian SLAM formulation.

A. Mathematical Representation of the Feature Map

This section demonstrates that, in the context of jointly estimating the number of features and their locations, the collection of features, which is referred to as the feature map, is naturally represented by a finite set. The rationale behind this representation traces back to a fundamental consideration in estimation theory—estimation error. Without a meaningful notion of estimation error, estimation has very little meaning. Despite the fact that mapping error is equally as important as localization error, its formal treatment has been largely neglected. To illustrate this point, recall that in existing SLAM formulations, the map is constructed by stacking features into a vector and consider the simplistic scenarios depicted in Fig. 1.

Fig. 1(a) depicts a scenario in which there are two true features at coordinates $(0, 0)$ and $(1, 1)$. The true map M is then represented by the vector $M = [0\ 0\ 1\ 1]^T$. If features are stacked into a vector in order of appearance then, given a vehicle trajectory $X_{0:k}$ (e.g., as shown in the figure) and perfect measurements, the estimated map may be given by the vector $\hat{M} = [1\ 1\ 0\ 0]^T$. Despite a seemingly perfect estimate of the map, the Euclidean error of the estimated map $\|M - \hat{M}\|$ is 2. This inconsistency arises because the ordering of the features in the representation of the map should not be relevant. A vector representation, however, imposes a mathematically strict arrangement of features in the estimated map based on the order in which they

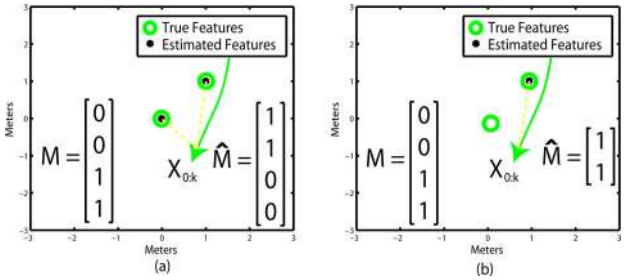

Fig. 1. Hypothetical scenario showing a fundamental inconsistency with vector representations of feature maps. If M is the true map, how should the error be assigned when the number of features in the map estimate $\hat{M}$ is incorrect?

were detected [1], [5]. Intuitively, the elements of $\hat{M}$ could be permuted to obtain a zero error; however, the representation of all possible permutations of the elements of a vector is, by definition, a set. Hence, such a permuting operation implies that the resulting error distance is no longer a distance for vectors but a distance for sets, and thus, this paper derives a set-based approach to SLAM. Another problem is depicted in Fig. 1(b), in which there are again two features at (0,0) and (1,1), but due to a missed detection (for instance), the estimated map comprises only one feature at (1,1). In such a situation, it is difficult to define a mathematically consistent error metric, i.e., Euclidean error and mean-squared error (MSE), between the vectors M and $\hat{M}$ since they contain a different number of elements. It is evident from these examples that stacking individual features into a single vector does not lead to a natural notion of mapping error, in general.

A *finite set* representation of the map $\mathcal{M}_k = \{m_k^1, \ldots, m_k^{\mathfrak{m}_k}\}$, where $m_k^1, \ldots, m_k^{\mathfrak{m}_k}$ are the $\mathfrak{m}_k$ features present at time k, admits a natural notion of estimation error since the "distance," or error between sets, is a well-understood concept, for example, the Hausdorff, optimal mass transfer (OMAT) [12], and optimal subpattern assignment (OSPA) [13], distances.

It should be noted that, while finite sets naturally capture the intrinsic properties of a feature map, a finite set map representation for grid-based frameworks [14], is unnecessary since the number of grid cells is known (*a priori* tessellation), and the order of the map states signifies their spatial location in the grid. As such, grid-map-estimation errors can be readily defined via Euclidean, mean squared, or sum of squared error metrics [15]. Due to the fundamentally different estimation state space of grid maps, being in occupancy space, it is difficult to draw comparison between grid-based SLAM algorithms and the RFS feature-based framework proposed in this paper.

For most sensor models considered in SLAM, the order in which sensor readings are recorded at each sampling instance simply depends on the direction in which the vehicle/sensor points and has no significance on the state of the map, which typically evolves in a globally defined coordinate system, independent of the vehicle's pose. Moreover, the number of measurements $\mathfrak{z}_k$ at any given time is not fixed due to detection uncertainty, spurious measurements, and unknown number of features. Thus, this type of measurement may also be naturally represented by a *finite set* of readings $\mathcal{Z}_k = \{z_k^1, z_k^2, \ldots, z_k^{\mathfrak{z}_k}\}$.

B. Random Finite Set–Simultaneous Localization and Mapping

This section outlines the RFS–SLAM model followed by the Bayesian RFS–SLAM filter.

1) Random Finite Set–Simultaneous Localization and Mapping Model: In the Bayesian estimation paradigm, the states/parameters and measurements are treated as realizations of random variables. Since the map (and the measurement) is more appropriately represented by a finite set, in such a framework, the concept of an RFS is required for Bayesian map estimation, [9]. Similar to a random vector being a vector-valued random variable (vehicle trajectory for instance), an RFS is simply a finite-set-valued random variable. Moreover, similar to random vectors, the probability density (if it exists) is a very useful descriptor of an RFS, especially in filtering and estimation. However, the space of finite sets does not inherit the usual Euclidean notion of integration and density. Hence, standard tools for random vectors are not appropriate for RFSs. Mahler's finite-set statistics (FISST) provide practical mathematical tools to deal with RFSs [16], [17], which is based on a notion of integration and density that is consistent with point-process theory [18]. This approach has attracted substantial research interest in the multitarget tracking community [19], with a more comprehensive list of applications appearing in [15]. An informal introduction to RFS estimation can be found in [20], with a detailed description of the latest advances available in [21] and [22].

Letting $\mathcal{M}$ be the RFS representing the entire unknown and unexplored static map and $\mathcal{M}_{k-1}$ be the RFS representing the subset of that map that has been explored, i.e., that has passed through the FoV of the vehicle mounted sensor, i.e.,

$$\mathcal{M}_{k-1} = \mathcal{M} \cap \mathrm{FoV}(X_{0:k-1}). \tag{1}$$

Note that $\mathrm{FoV}(X_{0:k-1}) = \mathrm{FoV}(X_0) \cup \mathrm{FoV}(X_1) \cup \ldots \cup \mathrm{FoV}(X_{k-1})$. $\mathcal{M}_{k-1}$, therefore, represents the set on the space of features that intersects with the union of individual FoVs, over the vehicle trajectory up to and including time $k-1$. Given this representation, the explored map $\mathcal{M}_{k-1}$ evolves in time according to

$$\mathcal{M}_k = \mathcal{M}_{k-1} \cup (\mathrm{FoV}(X_k) \cap \bar{\mathcal{M}}_{k-1}) \tag{2}$$

where $\bar{\mathcal{M}}_{k-1} = \mathcal{M} - \mathcal{M}_{k-1}$ (note the difference operator used here is the set difference), i.e., the set of features that are not in $\mathcal{M}_{k-1}$. Letting the new features that have entered the FoV, i.e., the second term of (2), be modeled by the independent RFS $\mathcal{B}_k(X_k)$, in this case, the RFS map-transition density is given by,

$$f_{\mathcal{M}}(\mathcal{M}_k|\mathcal{M}_{k-1}, X_k) = \sum_{\mathcal{W} \subseteq \mathcal{M}_k} f_{\mathcal{M}}(\mathcal{W}|\mathcal{M}_{k-1}) f_{\mathcal{B}}(\mathcal{M}_k - \mathcal{W}|X_k) \tag{3}$$

where $f_{\mathcal{M}}(\mathcal{W}|\mathcal{M}_{k-1})$ is the transition density of the set of features that are in the $\mathrm{FoV}(X_{0:k-1})$ at time $k-1$ to time k, and $f_{\mathcal{B}}(\mathcal{M}_k - \mathcal{W}|X_k)$ is the density of the RFS $\mathcal{B}(X_k)$ of the new features that pass within the FoV at time k. Modeling the vehicle dynamics by the standard Markov process with transition density $f_X(X_k|X_{k-1}, U_k)$, where U_k denotes the control input

at time k, the joint transition density of the map and the vehicle pose can be written as

$$f_{k|k-1}(\mathcal{M}_k, X_k|\mathcal{M}_{k-1}, X_{k-1}, U_k) = f_{\mathcal{M}}(\mathcal{M}_k|\mathcal{M}_{k-1}, X_k) f_X(X_k|X_{k-1}, U_k). \quad (4)$$

The measurement $\mathcal{Z}_k$ received by the vehicle with pose X_k, at time k, can be modeled by

$$\mathcal{Z}_k = \bigcup_{m \in \mathcal{M}_k} \mathcal{D}_k(m, X_k) \cup \mathcal{C}_k(X_k) \quad (5)$$

where $\mathcal{D}_k(m, X_k)$ is the RFS of measurements generated by a feature at m and $\mathcal{C}_k(X_k)$ is the RFS of the spurious measurements at time k, which may depend on the vehicle pose X_k. Therefore, $\mathcal{Z}_k$ consists of a random number, $\mathfrak{z}_k$, of measurements, whose order of appearance has no physical significance with respect to the estimated map of features. It is also assumed that all $\mathcal{D}_k(m, X_k)$, and $\mathcal{C}_k(X_k)$ are independent RFSs when conditioned on X_k.

The RFS of the measurements generated by a feature at m can be modeled by a Bernoulli RFS[1] [17] given by $\mathcal{D}_k(m, X_k)=\emptyset$ with probability $1-p_D(m|X_k)$ and $\mathcal{D}_k(m, X_k)=\{z\}$ with probability density $p_D(m|X_k)g_k(z|m, X_k)$. For a given robot pose X_k, $p_D(m|X_k)$ is the probability of the sensor detecting a feature at m. Given a detection, $g_k(z|m, X_k)$ is then the likelihood that a feature at m generates the measurement z. The assumed Poisson RFS $\mathcal{C}_k(X_k)$ represents the spurious measurements, which may be dependent on the vehicle pose X_k.

Using finite-set statistics [9], the likelihood of the measurement $\mathcal{Z}_k$ is then given by

$$g_k(\mathcal{Z}_k|X_k, \mathcal{M}_k) = \sum_{\mathcal{W} \subseteq \mathcal{Z}_k} f_{\mathcal{D}}(\mathcal{W}|\mathcal{M}_k, X_k) f_{\mathcal{C}}(\mathcal{Z}_k - \mathcal{W}|X_k) \quad (6)$$

with $f_{\mathcal{D}}(\mathcal{W}|\mathcal{M}_k, X_k)$ denoting the density of the RFS of observations, and $f_{\mathcal{C}}(\mathcal{Z}_k - \mathcal{W}|X_k)$ denoting the density of the clutter RFS, i.e., $\mathcal{C}_k(X_k)$. It can be seen that this likelihood directly encapsulates the inherent measurement uncertainty, with $f_{\mathcal{D}}(\mathcal{W}|\mathcal{M}_k, X_k)$ considering detection uncertainty and measurement noises, and $f_{\mathcal{C}}(\mathcal{Z}_k - \mathcal{W}|X_k)$ modeling the spurious measurements. This density is typically *a priori* given as Poisson in number and uniform in space [3]. The Bayesian RFS–SLAM filter is outlined next.

2) Random Finite Set–Simultaneous Localization and Mapping Filter: Letting the joint posterior density of the map $\mathcal{M}_k$ be denoted by $p_k(\mathcal{M}_k, X_{1:k}|Z_{1:k}, U_{1:k}, X_0)$ and the vehicle trajectory by $X_{0:k}$, for clarity of exposition, the following abbreviations shall be adhered to:

$$p_{k|k-1}(\mathcal{M}_k, X_{1:k}) = p_{k|k-1}(\mathcal{M}_k, X_{1:k}|Z_{0:k}, U_{0:k-1}, X_0)$$
$$p_k(\mathcal{M}_k, X_{1:k}) = p_k(\mathcal{M}_k, X_{1:k}|Z_{0:k}, U_{0:k-1}, X_0).$$

[1]The Bernoulli RFS is empty with a probability $1-\epsilon$ and is distributed according to a density π with probability ϵ.

The recursion for a static feature map is then given as follows:

$$p_{k|k-1}(\mathcal{M}_k, X_{1:k}) = f_X(X_k|X_{k-1}, U_k) \times \int f_{\mathcal{M}}(\mathcal{M}_k|\mathcal{M}_{k-1}, X_k) p_{k-1}(\mathcal{M}_{k-1}, X_{1:k-1}) \delta\mathcal{M}_{k-1} \quad (7)$$

$$p_k(\mathcal{M}_k, X_{1:k}) = \frac{g_k(\mathcal{Z}_k|X_k, \mathcal{M}_k) p_{k|k-1}(\mathcal{M}_k, X_{1:k})}{g_k(\mathcal{Z}_k|\mathcal{Z}_{0:k-1}, X_0)} \quad (8)$$

where the δ denotes a set integral.[2]

The joint posterior density encapsulates all statistical information about the map and vehicle pose, that can be inferred from the measurements and control history up to time k. The RFS–SLAM recursion (8) integrates uncertainty in DA and the number of features into a single Bayesian filter and does not require a separate DA step or any form of feature management, as is classically required [5], [6], [8].

The outputs of a SLAM algorithm are the estimate of the vehicle trajectory and the map. In a Bayesian approach, these are computed from the joint posterior density in (8). The following section establishes Bayes optimality for various RFS–SLAM estimators, while Section IV presents a tractable solution of the RFS–SLAM recursion.

III. Bayes Optimal Random Finite Set–Simultaneous Localization and Mapping Estimators

This section discusses various Bayes estimators for the SLAM problem and their optimality, which are based on a vector representation of the vehicles trajectory, and a finite-set representation of the map. The notion of Bayes optimal estimators is fundamental to the Bayesian-estimation paradigm. In general, if the function $\hat{\theta} : z \mapsto \hat{\theta}(z)$ is an estimator of a parameter θ, which is based on a measurement z, and $C(\hat{\theta}(z), \theta)$ is the cost for using $\hat{\theta}(z)$ to estimate θ, then the Bayes risk $R(\hat{\theta})$ is the expected cost over all possible realizations of the measurement and parameter, i.e.,

$$R(\hat{\theta}) = \int \int C(\hat{\theta}(z), \theta) p(z, \theta) d\theta dz \quad (9)$$

where $p(z, \theta)$ is the joint probability density of the measurement z and the parameter θ. A Bayes optimal estimator is any estimator that minimizes the Bayes risk [23], [24].

In the SLAM context, relevant Bayes optimal estimators are those for the vehicle trajectory and the map. The posterior densities $p_k(X_{1:k}) \triangleq p_k(X_{1:k}|Z_{0:k}, U_{0:k-1}, X_0)$, and $p_k(\mathcal{M}_k) \triangleq p_k(\mathcal{M}_k|Z_{0:k}, U_{0:k-1}, X_0)$ for the vehicle trajectory and map, can be obtained by marginalizing the joint posterior density $p_k(\mathcal{M}_k, X_{1:k}|Z_{0:k}, U_{0:k-1}, X_0)$. For the vehicle trajectory, the posterior mean, which minimizes the MSE, is a widely used Bayes optimal estimator. However, since the map is more appropriately represented as a finite set, the notion of MSE does not apply. Moreover, standard Bayes optimal estimators are defined for vectors and, subsequently, do not apply to finite-set

[2]Since the integration variable (the map) is a finite set, the usual definition of integration for vectors does not apply. In this case, a set integral is required. For more details, see [17] and [18].

feature maps. To the best of the authors' knowledge, there is no work which establishes Bayes optimality of estimators for finite-set feature maps (and, consequently, feature-based SLAM in terms of taking the estimated number of features into account).

A. Optimal Feature-Map Estimation

In the following, as before, letting $\mathcal{M}_k$ denote the feature-based map state at time k comprising $\mathfrak{m}_k$ features, and $p_k(\mathcal{M}_k)$ denote its posterior spatial density. If $\hat{\mathcal{M}}_k : Z_{1:k} \mapsto \hat{\mathcal{M}}_k(Z_{1:k})$ is an estimator of the feature map $\mathcal{M}_k$, and $C(\hat{\mathcal{M}}_k(Z_{1:k}), \mathcal{M}_k)$ is the cost for using $\hat{\mathcal{M}}_k(Z_{1:k})$ to estimate $\mathcal{M}_k$, then the Bayes risk for mapping is given by

$$R(\hat{\mathcal{M}}_k) = \int \int C(\hat{\mathcal{M}}_k(Z_{1:k}), \mathcal{M}_k) p_k(\mathcal{M}_k, Z_{1:k}) \delta\mathcal{M}_k \delta\mathcal{Z}_{1:k} \tag{10}$$

where $p_k(\mathcal{M}_k, Z_{1:k})$ is the joint density of the map and measurement history. Since, due to the arguments presented in Section II-A, the map and measurements are more appropriately represented as sets, the Bayes risk above is defined in terms of set integrals. Several principled solutions to performing feature map estimation such as the joint multiobject estimator or marginal multiobject estimator [17] can be applied, as can the PHD estimator, which is next described and adopted in this paper.

B. Probability Hypothesis Density Estimator

An intuitive approach to RFS state estimation is to exploit the physical interpretation of the first moment of an RFS, which is its PHD, i.e., v_k [17]. For a map RFS $\mathcal{M}_k$, the PHD is a nonnegative function v, such that for each region S in the space of features

$$\int_S v_k(m) dm = \mathbb{E}[|\mathcal{M}_k \cap S|]. \tag{11}$$

The mass of the PHD gives the expected number of features $\hat{\mathfrak{m}}_k$ in the map $\mathcal{M}_k$, and its peaks indicate locations with high probability of feature existence. A discussion on the optimality/suboptimality of the PHD estimator is provided in [22].

If the RFS $\mathcal{M}_k$ is Poisson, i.e., the number of points is Poisson distributed and the points themselves are independently and identically distributed (iid), then the probability density of $\mathcal{M}_k$ can be constructed exactly from the PHD,

$$p(\mathcal{M}_k) = \frac{\prod_{m \in \mathcal{M}_k} v_k(m)}{\exp(\int v_k(m) dm)}. \tag{12}$$

In this sense, the PHD can be thought of as a first-moment approximation of the probability density of an RFS.

IV. Probability Hypothesis Density–Simultaneous Localization and Mapping Filter

Since the full RFS–SLAM filter is numerically intractable, it is necessary to look for tractable but principled approximations. The PHD approach which propagates the first-order moment of the posterior multitarget RFS has proven to be both powerful and effective in multitarget filtering [17]. However, this technique cannot be directly applied to SLAM that propagates the joint posterior density of the map and the vehicle trajectory.

This section derives a recursion that jointly propagates the posterior PHD of the map and the posterior density of the vehicle trajectory. Analogous to FastSLAM, the RFS–SLAM recursion can be factorized as shown in Section IV-A. Section IV-B discusses the PHD estimator in the context of this factorized recursion. Section IV-D presents a trajectory-conditioned mapping algorithm based on the PHD, while Section IV-E extends this mapping algorithm to perform SLAM.

A. Factorized RFS-SLAM

Using standard conditional probability, the joint posterior RFS–SLAM density of (8) can be decomposed as

$$\begin{aligned} &p_k(\mathcal{M}_k, X_{1:k} | \mathcal{Z}_{0:k}, U_{0:k-1}, X_0) \\ &\quad = p_k(X_{1:k} | \mathcal{Z}_{0:k}, U_{0:k-1}, X_0) p_k(\mathcal{M}_k | \mathcal{Z}_{0:k}, X_{0:k}). \end{aligned} \tag{13}$$

Thus, the recursion for the joint RFS map-trajectory posterior density according to (8) is equivalent to jointly propagating the posterior density of the map conditioned on the trajectory and the posterior density of the trajectory. In this section, as before, for compactness

$$\begin{aligned} p_{k|k-1}(\mathcal{M}_k | X_{0:k}) &= p_{k|k-1}(\mathcal{M}_k | \mathcal{Z}_{0:k-1}, X_{0:k}) \\ p_k(\mathcal{M}_k | X_{0:k}) &= p_k(\mathcal{M}_k | \mathcal{Z}_{0:k}, X_{0:k}) \\ p_k(X_{1:k}) &= p_k(X_{1:k} | \mathcal{Z}_{0:k}, U_{0:k-1}, X_0) \end{aligned}$$

and it follows that

$$\begin{aligned} p_{k|k-1}(\mathcal{M}_k | X_{0:k}) &= \int f_{\mathcal{M}}(\mathcal{M}_k | \mathcal{M}_{k-1}, X_k) \\ &\quad \times p_{k-1}(\mathcal{M}_{k-1} | X_{0:k-1}) \delta\mathcal{M}_{k-1} \end{aligned} \tag{14}$$

$$p_k(\mathcal{M}_k | X_{0:k}) = \frac{g_k(\mathcal{Z}_k | \mathcal{M}_k, X_k) p_{k|k-1}(\mathcal{M}_k | X_{0:k})}{g_k(\mathcal{Z}_k | \mathcal{Z}_{0:k-1}, X_{0:k})} \tag{15}$$

$$\begin{aligned} p_k(X_{1:k}) &= g_k(\mathcal{Z}_k | \mathcal{Z}_{0:k-1}, X_{0:k}) \\ &\quad \times \frac{f_X(X_k | X_{k-1}, U_{k-1}) p_{k-1}(X_{1:k-1})}{g_k(\mathcal{Z}_k | \mathcal{Z}_{0:k-1})}. \end{aligned} \tag{16}$$

Apart from adopting RFS likelihoods for the measurement and map, the recursion defined by (14)–(16) is similar to that in FastSLAM [6], [25]. However, the use of RFS likelihoods has important consequences in the evaluation of (16), as shown later in Section IV-E. In FastSLAM, it should be noted that the map recursion of (15) is further decomposed into the product of K independent densities for each of the K features assumed to exist in the map. Furthermore, FastSLAM is conditioned on the inherently unknown DA assignments. In contrast, RFS–SLAM is not conditioned on any DA hypotheses to determine the number of features to estimate, and the recursion of (15) is that of an RFS feature map. Consequently, the propagation of the map involves probability densities of RFS s and marginalization over the map involves set integrals. Similar to FastSLAM, the effect of the trajectory conditioning on RFS–SLAM is to render each feature estimate conditionally independent, and thus, the map correlations, which are critical to EKF–SLAM [5], are not required.

B. PHD in RFS-SLAM

Recall from Section III-A, that an optimal estimator for a random vector is the conditional expectation. Many state-of-the-art SLAM algorithms adopt sequential Monte Carlo (SMC) methods. It is well known that SMC techniques are more amenable to expectation operations than maximization operations, since if p is approximated by a set of weighted samples $\{w^{(i)}, X^{(i)}\}_{i=1}^{N}$, then [26], [27]

$$\sum_{i=1}^{N} w^{(i)} X^{(i)} \rightarrow \mathbb{E}[X] \tag{17}$$

as $N \rightarrow \infty$. However, in FastSLAM [6], it is common to choose the trajectory sample with the highest weight as the estimate of the vehicle path, and its corresponding map, as the estimate of the map. It is easier to establish convergence in SMC implementations if we use the expected path and expected map. However, it is not clear how the expected map is interpreted.

The PHD construct allows an alternative notion of expectation for maps, thereby fully exploiting the advantage of an SMC approximation. The PHD v is a function defined on the feature space satisfying (11). The value of the PHD at a point gives the expected number of features at that point, while the integral over any given region gives the expected number of features in that region. A salient property of the PHD construct in map estimation is that the posterior PHD of the map is indeed the expectation of the trajectory-conditioned PHDs. More concisely

$$v_k(m) = \mathbb{E}\left[v_k(m|X_{1:k})\right] \tag{18}$$

where the expectation is taken over the vehicle trajectory $X_{1:k}$. This result follows from standard properties of the PHD (intensity function) of an RFS; see, for example, classical texts such as [28] and [29]. Thus, the PHD construct provides a natural framework to average feature-map estimates, while incorporating both unknown associations and different feature numbers. This differs dramatically from vector-based map-averaging methods which require feature identification tracking and rule-based combinations [30]. In contrast, map averaging for grid-based maps is straightforward due to both known grid alignments and number of cells. While the practical merits of an expected feature map estimate for SLAM using a single sensor may be unclear at this time, related operations such as "feature-map addition" may be of use in sensor fusion and multirobot SLAM applications. Furthermore, the PHD construct admits a Bayes optimal estimator for the map, as discussed in Section III-A.

C. Evidence Grids and the Probability Hypothesis Density

As mentioned in Section I, the PHD of a map is closely related to the occupancy-grid representation. Intuitively, the PHD can be interpreted as a limiting case of the occupancy probability. Following [31], considering a grid system, and letting m_i, $B(m_i)$ denote the center and region defined by the boundaries of the ith grid cell. Let $P^{(occ)}(B(m_i))$ and $\lambda(B(m_i))$ denote the occupancy probability and the area of the ith grid cell. Assuming that the grid is sufficiently fine so that each grid cell contains at most one feature, then the expected number of features over the region $S_J = \bigcup_{i\in J} B(m_i)$ is given by

$$\begin{aligned}\mathbb{E}\left[|M \cap S_J|\right] &= \sum_{i\in J} P^{(occ)}(B(m_i)) \\ &= \sum_{i\in J} v(m_i)\lambda(B(m_i))\end{aligned}$$

where $v(m_i) = \frac{P^{(occ)}(B(m_i))}{\lambda(B(m_i))}$. Intuitively, as the grid cell area tends to zero (or for an infinitesimally small cell), any region S can be approximated by $\bigcup_{i\in J} B(m_i)$ for some J. The sum then becomes an integral and the expected number of features in S becomes

$$\mathbb{E}\left[|M \cap S|\right] = \int_S v(m)dm. \tag{19}$$

Hence, the PHD $v(m)$ can be interpreted as the occupancy probability density at the point m. The recursive propagation of the PHD is discussed in the following section.

D. Probability Hypothesis Density Mapping

This section details the trajectory-conditioned PHD-mapping recursion of (15), as was first proposed in [10]. The predicted and posterior RFS maps are approximated by Poisson RFSs with PHDs $v_{k|k-1}(m|X_{0:k})$ and $v_k(m|X_{0:k})$, respectively

$$p_{k|k-1}(\mathcal{M}_k|X_{0:k}) \approx \frac{\prod_{m\in\mathcal{M}_k} v_{k|k-1}(m|X_{0:k})}{\exp\left(\int v_{k|k-1}(m|X_{0:k})dm\right)} \tag{20}$$

$$p_k(\mathcal{M}_k|X_{0:k}) \approx \frac{\prod_{m\in\mathcal{M}_k} v_k(m|X_{0:k})}{\exp\left(\int v_k(m|X_{0:k})dm\right)}. \tag{21}$$

In essence, this approximation assumes that features are iid and the number of features is Poisson distributed. This PHD approximation has been proven to be powerful and effective in multitarget tracking [17]. Poisson approximations for the number of new features have also been adopted in certain SLAM solutions [3].

Under these approximations, it has been shown [3] that, similar to standard recursive estimators, the PHD recursion has a *predictor–corrector* form. The PHD predictor equation is

$$v_{k|k-1}(m|X_{0:k}) = v_{k-1}(m|X_{0:k-1}) + b(m|X_k) \tag{22}$$

where $b(m|X_k)$ is the PHD of the new feature RFS, i.e., $\mathcal{B}(X_k)$, as discussed previously in Section II-B. The PHD corrector equation is then

$$\begin{aligned}v_k(m|X_{0:k}) = v_{k|k-1}(m|X_{0:k})\Bigg[1 - P_D(m|X_k) \\ + \sum_{z\in\mathcal{Z}_k} \frac{\Lambda(m|X_k)}{c_k(z|X_k) + \int \Lambda(\zeta|X_k)v_{k|k-1}(\zeta|X_{0:k})d\zeta}\Bigg]\end{aligned} \tag{23}$$

where $\Lambda(m|X_k) = P_D(m|X_k)g_k(z|m, X_k)$, and

$$\begin{aligned}P_D(m|X_k) &= \text{the probability of detecting a feature at } m, \text{ from vehicle pose } X_k \\ c_k(z|X_k) &= \text{PHD of the clutter RFS } \mathcal{C}_k \text{ in (5) at time } k.\end{aligned}$$

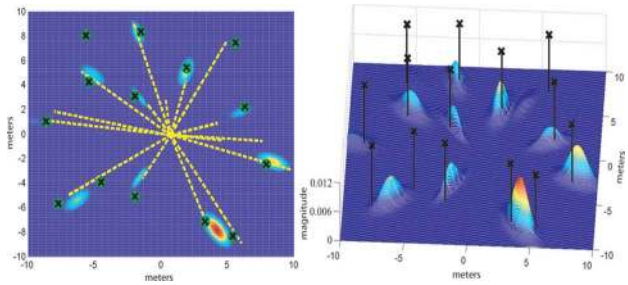

Fig. 2. Sample map PHD at time $k-1$, with the true map represented by black crosses. The measurement at $k-1$ is represented by the yellow dashed lines. The peaks of the PHD represent locations with highest concentration of expected number of features. The local PHD mass in the region of most features is 1, thus indicating the presence of one feature. The local mass close to some unresolved features (for instance at (5,–8)) is closer to 2, thereby demonstrating the unique ability of the PHD function to jointly capture the number of features.

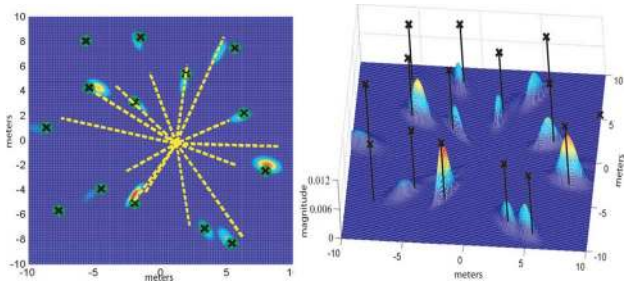

Fig. 3. Map PHD from Fig. 2 and the measurement at time k. Note that the features at (5,–8) are resolved due to well-separated measurements, while at (–1,–4), a lone false alarm close to the feature measurement contributes to the local PHD mass. At (–5,–4), a small likelihood over all measurements, coupled with a moderate $c_k(z|X_k)$, results in a reduced local mass.

The predictor of (22) comprises the sum of the previous PHD and the PHD of the set of static features hypothesized to enter the sensor's FoV due to vehicle motion. The corrector of (23) is governed by the following sensor characteristics [17].

1) $P_D(m|X_k)$. If a feature at m is not in $\mathrm{FoV}(X_k)$, it could not have been observed; thus, $P_D(m|X_k)=0$. From (23)

$$v_k(m|X_{0:k}) = v_{k|k-1}(m|X_{0:k})[1-0+0]$$

i.e., the updated PHD equals the predicted PHD, as no new information is available. On the other hand, if m is in $\mathrm{FoV}(X_k)$ and $P_D(m|X_k)\approx 1$, the summation over all measurements tends to dominate. Then, the predicted PHD is modified by the sum of terms dependent on the measurement likelihood and clutter PHD.

2) $c_k(z|X_k)$. A particular measurement could have originated from a feature or a false alarm. Assuming $P_D(m|X_k)$ is constant and the number of false alarms is large and uniformly distributed in the region $\mathrm{FoV}(X_k)$, the summation term of (23) is then dominated by $c_k(z|X_k)$. Since the measurement is likely to be a false alarm, it contributes little to the total posterior feature count, as it should. On the other hand, if the number of false alarms is low, $c_k(z|X_k)$ dominates less, and the measurement contributes more to the value of the posterior PHD.

3) $g_k(z|m,X_k)$. Let us assume that the sensor model is accurate, thus $g_k(z|m,X_k)$ is large for the m, which produces z. If z is consistent with prior information (the observation model), the numerator will dominate the summation of (23). Conversely, if $g_k(z|m,X_k)$ is small, and the measurement is unlikely to be from m, its corresponding term in the summation will have little influence.

A graphical depiction of a the posterior PHD after two consecutive measurements, approximated by a Gaussian mixture (GM), is shown, respectively, in Figs. 2 and 3.

The PHD recursion is far more numerically tractable than propagating the RFS map densities of (15). In addition, the recursion can be readily extended to incorporate multiple sensors/vehicles by sequentially updating the map PHD with the measurement from each robot.

E. Probability Hypothesis Density–Simultaneous Localization and Mapping

This section extends the trajectory-conditioned PHD mapping recursion to the SLAM problem. With the hindsight of FastSLAM [6], the most obvious extension of PHD mapping [10] to SLAM is to exploit the factorization (14)–(16), e.g., PHD for mapping and particle filtering for localization. This technique requires the computation of the posterior density of the vehicle trajectory in (16), in particular, the term $g_k(\mathcal{Z}_k|\mathcal{Z}_{0:k-1},X_{0:k})$, which requires set integration

$$g_k(\mathcal{Z}_k|\mathcal{Z}_{0:k-1},X_{0:k}) = \int p(\mathcal{Z}_k,\mathcal{M}_k|\mathcal{Z}_{0:k-1},X_{0:k})\delta M_k. \tag{24}$$

This set integral is numerically intractable and a naive approach is to directly apply the EKF approximation proposed for FastSLAM [32]. However, an EKF approximation cannot be used since the likelihood (24), which is defined on the space of finite sets, and its FastSLAM counterpart, which is defined on a Euclidean space, are two fundamentally different quantities and it is not known how they are even related. Therefore, in this case, it is fundamentally incorrect to use the EKF approximation in [6], as it will not result in a valid density, and thus, its product with (15) cannot give the joint posterior of the map and pose.

Fortunately, by rearranging (15), it can be seen that $g_k(\mathcal{Z}_k|\mathcal{Z}_{0:k-1},X_{0:k})$ is merely the normalizing constant

$$g_k(\mathcal{Z}_k|\mathcal{Z}_{0:k-1},X_{0:k}) = \frac{g_k(\mathcal{Z}_k|\mathcal{M}_k,X_k)p_{k|k-1}(\mathcal{M}_k|X_{0:k})}{p_k(\mathcal{M}_k|X_{0:k})}. \tag{25}$$

Note in the above, that the LHS does not contain the variable $\mathcal{M}_k$, while the RHS has $\mathcal{M}_k$ in both the denominator and numerator. In essence, $\mathcal{M}_k$ in (25) is a dummy variable, and thus, (25) holds for any arbitrary choice of $\mathcal{M}_k$. This allows the substitution of any choice of $\mathcal{M}_k$ to evaluate $g_k(\mathcal{Z}_k|\mathcal{Z}_{0:k-1},X_{0:k})$. This is an important result, which allows for the likelihood of the measurement-conditioned on the trajectory (but not the map), to be calculated in closed-form, as opposed to using the EKF approximations in [6]. The following considers two simple choices.

1) Empty Map: Setting $\mathcal{M}_k = \emptyset$, and using the Poisson RFS approximations, i.e., (20) and (21), as well as the RFS measurement likelihood, i.e., (6), it follows that (see Appendix A)

$$g_k(\mathcal{Z}_k|\mathcal{Z}_{0:k-1}, X_{0:k}) \approx \kappa_k^{\mathcal{Z}_k} \times \exp\left(\hat{\mathfrak{m}}_k - \hat{\mathfrak{m}}_{k|k-1} - \int c_k(z|X_k)dz\right) \quad (26)$$

where $\kappa_k^{\mathcal{Z}_k} = \prod_{z\in\mathcal{Z}_k} c_k(z|X_k)$, with $c_k(z|X_k)$ being the PHD of the measurement clutter RFS $\mathcal{C}_k(X_k)$. In addition, $\hat{\mathfrak{m}}_k = \int v_k(m|X_{0:k})dm$, and $\hat{\mathfrak{m}}_{k|k-1} = \int v_{k|k-1}(m|X_{0:k})dm$.

2) Single-Feature Map: In a similar manner, to evaluate the normalizing constant for the case of $\mathcal{M}_k = \{\bar{m}\}$, again using (6), (20), and (21)

$$g_k(\mathcal{Z}_k|\mathcal{Z}_{0:k-1}, X_{0:k}) \approx \frac{1}{\Gamma}\left[\left((1 - P_D(\bar{m}|X_k))\kappa_k^{\mathcal{Z}_k} + P_D(\bar{m}|X_k)\sum_{z\in\mathcal{Z}_k}\kappa_k^{\mathcal{Z}_k-\{z\}}g_k(z|\bar{m}, X_k)\right)v_{k|k-1}(\bar{m}|X_{0:k})\right] \quad (27)$$

with

$$\Gamma = \exp\left(\hat{\mathfrak{m}}_{k|k-1} - \hat{\mathfrak{m}}_k + \int c_k(z)dz\right)v_k(\bar{m}|X_{0:k}). \quad (28)$$

For this choice of $\mathcal{M}_k$, $\bar{m}$ can be, for instance, the feature with the least uncertainty or the maximum measurement likelihood. It is possible to choose $\mathcal{M}_k$ with multiple features; however, this will increase the computational burden. Due to the presence of the measurement likelihood term $g_k(z|\bar{m}, X_k)$, it is expected that, in general, the single-feature map update will outperform that of the empty-map update. Note that in (25), every choice of $\mathcal{M}_k$ would give the same result; however, (26) and (27) use different *approximations* of $p_k(\mathcal{M}_k|X_{0:k})$, thus yielding slightly different results. The following section presents an RB implementation of the proposed PHD–SLAM filter.

V. Rao–Blackwellized Implementation of the PHD-SLAM Filter

Following the description of the PHD–SLAM filter in the previous section, an RB implementation is detailed in this section. In essence, a particle filter is used to propagate the vehicle trajectory in (16), and a GM PHD filter is used to propagate each trajectory-conditioned map PHD in (15). As such, letting the PHD–SLAM density at time $k-1$ be represented by a set of N particles

$$\left\{w_{k-1}^{(i)}, X_{0:k-1}^{(i)}, v_{k-1}^{(i)}(m|X_{0:k-1}^{(i)})\right\}_{i=1}^{N}$$

where $X_{0:k-1}^{(i)} = [X_0, X_1^{(i)}, X_2^{(i)}, \ldots, X_{k-1}^{(i)}]$ is the ith hypothesized vehicle trajectory, and $v_{k-1}^{(i)}(m|X_{0:k-1}^{(i)})$ is its map PHD. The filter then proceeds to approximate the posterior density by a new set of weighted particles

$$\left\{w_k^{(i)}, X_{0:k}^{(i)}, v_k^{(i)}(m|X_{0:k}^{(i)})\right\}_{i=1}^{N}$$

as follows.

A. PHD Mapping

Let the prior map PHD for the ith particle $v_{k-1}^{(i)}(m|X_{k-1}^{(i)})$ be a GM of the form

$$v_{k-1}(m|X_{k-1}^{(i)}) = \sum_{j=1}^{J_{k-1}^{(i)}} \eta_{k-1}^{(i,j)}\mathcal{N}\big(m; \mu_{k-1}^{(i,j)}, P_{k-1}^{(i,j)}\big) \quad (29)$$

which is a mixture of $J_{k-1}^{(i)}$ Gaussians, with $\eta_{k-1}^{(i,j)}$, $\mu_{k-1}^{(i,j)}$, and $P_{k-1}^{(i,j)}$ being the corresponding predicted weights, means, and covariances, respectively, for the jth Gaussian component of the map PHD of the ith trajectory. Let the new feature intensity $b(m|\mathcal{Z}_{k-1}, X_k^{(i)})$ for the sampled pose $X_k^{(i)}$ at time k also be a GM of the form

$$b(m|\mathcal{Z}_{k-1}, X_k^{(i)}) = \sum_{j=1}^{J_{b,k}^{(i)}} \eta_{b,k}^{(i,j)}\mathcal{N}\big(m; \mu_{b,k}^{(i,j)}, P_{b,k}^{(i,j)}\big) \quad (30)$$

where $J_{b,k}^{(i)}$ defines the number of Gaussians in the new feature intensity at time k, and $\eta_{b,k}^{(i,j)}$, $\mu_{b,k}^{(i,j)}$, and $P_{b,k}^{(i,j)}$ are the corresponding components. This is analogous to the proposal distribution in the particle filter and provides an initial estimate of the new features entering the map.

The predicted intensity is therefore also a GM

$$v_{k|k-1}(m|X_k^{(i)}) = \sum_{j=1}^{J_{k|k-1}^{(i)}} \eta_{k|k-1}^{(i,j)}\mathcal{N}\big(m; \mu_{k|k-1}^{(i,j)}, P_{k|k-1}^{(i,j)}\big) \quad (31)$$

which consists of $J_{k|k-1}^{(i)} = J_{k-1}^{(i)} + J_{b,k}^{(i)}$ Gaussians representing the union of the prior map intensity $v_{k-1}(m|X_{k-1}^{(i)})$ and the proposed new feature intensity, according to (22). Since the measurement likelihood is also of Gaussian form, it follows from (23) that the posterior map PHD $v_k(m|X_k^{(i)})$ is then also a GM given by

$$v_k(m|X_k^{(i)}) = v_{k|k-1}(m|X_k^{(i)})\left[1 - P_D(m|X_k^{(i)}) + \sum_{z\in\mathcal{Z}_k}\sum_{j=1}^{J_{k|k-1}^{(i)}} v_{G,k}^{(i,j)}(z, m|X_k^{(i)})\right]. \quad (32)$$

The components of the above equation are given by

$$v_{G,k}^{(i,j)}(z, m|X_k^{(i)}) = \eta_k^{(i,j)}(z|X_k^{(i)})\mathcal{N}(m; \mu_{k|k}^{(i,j)}, P_{k|k}^{(i,j)}) \quad (33)$$

$$\eta_k^{(i,j)}(z|X_k^{(i)}) = \frac{P_D(m|X_k^{(i)})\eta_{k|k-1}^{(i,j)}q^{(i,j)}(z, X_k^{(i)})}{c(z) + \sum_{\ell=1}^{J_{k|k-1}^{(i)}} P_D(m|X_k^{(i)})\eta_{k|k-1}^{(i,\ell)}q^{(i,\ell)}(z, X_k^{(i)})} \quad (34)$$

where $q^{(i,j)}(z, X_k^{(i)}) = \mathcal{N}\big(z; H_k\mu_{k|k-1}^{(i,j)}, S_k^{(i,j)}\big)$. The terms $\mu_{k|k}$, $P_{k|k}$, and S_k can be obtained using any standard filtering technique such as extended Kalman filter (EKF) or unscented Kalman filter. In this paper, the EKF updates are adopted.

The clutter RFS, i.e., C_k, is assumed to be Poisson-distributed [3] in number and is uniformly spaced over the mapping region. Therefore, the clutter intensity is given by, $c(z) = \lambda_c \mathcal{U}(z)$, where λ_c is the average number of clutter measurements, and $\mathcal{U}(z)$ denotes a uniform distribution on the measurement space. As with other feature-based GM implementations [33], pruning and merging operations are required to curb the explosive growth in the number of Gaussian components of the posterior map PHD. These operations are carried out as in [34].

B. Vehicle Trajectory

The proposed filter adopts a particle approximation of the posterior vehicle trajectory, $p_k(X_{1:k})$, which is sampled/re-sampled as follows:

Step 1: *Sampling step*

1) For $i = 1, ..., N$, sample $\widetilde{X}_k^{(i)} \sim f_X(\widetilde{X}_k^{(i)} | X_{k-1}^{(i)}, U_{k-1})$, and set

$$\widetilde{w}_k^{(i)} = \frac{g_k(\mathcal{Z}_k | \mathcal{Z}_{0:k-1}, \widetilde{X}_{0:k}^{(i)}) f_X(\widetilde{X}_k^{(i)} | X_{k-1}^{(i)}, U_{k-1})}{f_X(\widetilde{X}_k^{(i)} | X_{k-1}^{(i)}, U_{k-1})} w_{k-1}^{(i)}.$$

2) Normalize weights : $\sum_{i=1}^{N} \widetilde{w}_k^{(i)} = 1$.

Step 2: *Resampling step*

1) Resample $\left\{ \widetilde{w}_k^{(i)}, \widetilde{X}_{0:k}^{(i)} \right\}_{i=1}^{N}$ to get $\left\{ w_k^{(i)}, X_{0:k}^{(i)} \right\}_{i=1}^{N}$.

Since the vehicle transition density is chosen as the proposal density as with FastSLAM 1.0 [6] then

$$\widetilde{w}_k^{(i)} = g_k(\mathcal{Z}_k | \mathcal{Z}_{0:k-1}, \widetilde{X}_{0:k}^{(i)}) w_{k-1}^{(i)} \tag{35}$$

which can be evaluated in closed form according to (26) or (27), where

$$\hat{\mathfrak{m}}_{k|k-1}^{(i)} = \sum_{j=1}^{J_{k|k-1}^{(i)}} \eta_{k|k-1}^{(i,j)} \quad \text{and} \quad \hat{\mathfrak{m}}_k^{(i)} = \sum_{j=1}^{J_k^{(i)}} \eta_k^{(i,j)}. \tag{36}$$

Note that the incorporation of the measurement-conditioned proposal of FastSLAM 2.0 can also be accommodated in this framework. That direction of research focuses on more efficient SMC approximations and is an avenue for further studies.

C. State Estimation and Pseudocode

As alluded to throughout this paper, in contrast to previous SLAM algorithms, the PHD-map representation allows for a natural ability to average feature maps, i.e., independent-map estimates from *N* independent trajectory particles can be readily averaged into an expected estimate, even with map estimates of different size and without having to resolve the intramap feature associations. Consequently, in the case of the RB–PHD–SLAM filter, both the expected vehicle trajectory and feature map can be determined as follows.

Given the posterior set of weighted particles and corresponding map PHDs

$$\left\{ w_k^{(i)}, X_{0:k}^{(i)}, v_k^{(i)}(m | X_{0:k}^{(i)}) \right\}_{i=1}^{N}$$

TABLE I
RB–PHD-FILTER: PREDICTION

1. **Given** $\{w_{k-1}^{(i)}, X_{k-1}^{(i)}, v_{k-1}^{(i)}\}_{i=1}^{N}$, $v_{k-1}^{(i)} = \{\eta_{k-1}^{(i,j)}, \mu_{k-1}^{(i,j)}, P_{k-1}^{(i,j)}\}_{j=1}^{J_{k-1}^{(i)}}$
2. **For** $i = 1, \ldots, N$
3. **Step 1** (Predict pose)
4. $\quad \widetilde{X}_k^{(i)} \sim f_X(X_k | X_{0:k-1}^{(i)}, U_{0:k-1}, X_0)$
5. **Step 2** (Predict map PHD given $\widetilde{X}_k^{(i)}$)
6. $\quad l = 0$
7. $\quad$ for $j = 1, \ldots, J_{b,k}^{(i)}$ (new Gaussian components)
8. $\quad\quad l = l + 1$
9. $\quad\quad \eta_{k|k-1}^{(i,l)} = \eta_{b,k}^{(i,j)},\ \mu_{k|k-1}^{(i,l)} = \mu_{b,k}^{(i,j)},\ P_{k|k-1}^{(i,l)} = P_{b,k}^{(i,j)}$
10. $\quad$ end
11. $\quad$ for $j = 1, \ldots, J_{k-1}^{(i)}$ (existing Gaussian components)
12. $\quad\quad l = l + 1$
13. $\quad\quad \eta_{k|k-1}^{(i,l)} = \eta_{k-1}^{(i,j)}, \mu_{k|k-1}^{(i,l)} = \mu_{k-1}^{(i,j)}, P_{k|k-1}^{(i,l)} = P_{k-1}^{(i,j)}$
14. $\quad$ end
15. $\quad J_{k|k-1}^{(i)} = l,\ \hat{\mathfrak{m}}_{k|k-1}^{(i)} = \sum_{j=1}^{J_{k|k-1}^{(i)}} \eta_{k|k-1}^{(i,j)}$
16. **End**

and $\bar{w} = \sum_{i=1}^{N} w_k^{(i)}$, then

$$\hat{X}_{0:k} = \frac{1}{\bar{w}} \sum_{i=1}^{N} w_k^{(i)} X_{0:k}^{(i)}. \tag{37}$$

As demonstrated previously in Section IV-B, the posterior PHD of the map is the expectation of the trajectory-conditioned PHDs, and thus

$$v_k(m | X_{0:k}) = \frac{1}{\bar{w}} \sum_{i=1}^{N} w_k^{(i)} v_k(m | X_{0:k}^{(i)}). \tag{38}$$

If $\hat{\mathfrak{m}}_k = \int v_k(m | X_{0:k}) dm$ is the mass of the posterior map PHD, the expected map estimate can then be extracted by choosing the $\hat{\mathfrak{m}}_k$ highest local maxima. The pseudocode for the RB–PHD–SLAM filter and expectation estimator are provided in Tables I–IV. The following section presents the results and analysis of the proposed filter.

VI. Results and Analysis

This section presents the results and analysis of the proposed approach using both simulated and experimental datasets. For comparative purposes, the benchmark algorithms used are the classical FastSLAM [6] with multiple hypothesis (MH) DA [35] and the joint compatibility branch and bound (JCBB) EKF [8]. The "single-feature-map" trajectory weighting of (27) is adopted for the proposed RB–PHD–SLAM filter, with an implementation using the "empty map update" of (26) appearing in [11]. While any feature can theoretically be selected to generate the trajectory weighting, in this implementation, that which generates the maximum likelihood (ML) amongst all measurements is chosen. A comprehensive study on the best-suited feature selection strategies is left for future work.

Current SLAM filters deal with clutter through "feature-management" routines, such as the landmark's quality [5], or a binary Bayes filter [6]. These operations are typically independent of the joint SLAM filter update, whereas the proposed

TABLE II
RB–PHD-FILTER: MAP UPDATE

1. **For** $i = 1, \ldots, N$
2. **Step 1** (Compute Update Terms)
3. for $j = 1, \ldots, J_{k|k-1}^{(i)}$
4. $\hat{z}^{(i,j)} = H_k[X_k^{(i)}\ \mu_{k|k-1}^{(i,j)}]^T$
5. $S_k^{(i,j)} = \nabla H_k P_{k|k-1}^{(i,j)}[\nabla H_k]^T + R$
6. $K_k^{(i,j)} = P_{k|k-1}^{(i,j)}[\nabla H_k]^T[S_k^{(i,j)}]^{-1}$
7. $P_{k|k}^{(i,j)} = [I - K_k^{(j)}\nabla H_k]P_{k|k-1}^{(i,j)}$
8. end
9. **Step 2** (Update GMM PHD Components)
10. for $j = 1, \ldots, J_{k|k-1}^{(i)}$ (missed detections)
11. $\eta_k^{(i,j)} = (1 - P_D)\eta_{k|k-1}^{(i,j)},\ \mu_k^{(i,j)} = \mu_{k|k-1}^{(i,j)},$ $P_k^{(i,j)} = P_{k|k-1}^{(i,j)}$
12. end
13. $l = 0$
14. for each $z \in \mathcal{Z}_k$ (detections)
15. $l = l + 1$
16. for $j = 1, \ldots, J_{k|k-1}^{(i)}$
17. $\tau^{(j)} = P_D\eta_{k|k-1}^{(i,j)}\mathcal{N}(z; \hat{z}^{(i,j)}, S_k^{(i,j)})$
18. $\mu_k^{(lJ_{k|k-1}^{(i)}+j)} = \mu_{k|k-1}^{(i,j)} + K_k^{(i,j)}(z - \hat{z}^{(i,j)})$
19. $P_k^{(lJ_{k|k-1}^{(i)}+j)} = P_{k|k}^{(i,j)}$
20. end
21. for $j = 1, \ldots, J_{k|k-1}^{(i)}$,
22. $\eta_k^{(lJ_{k|k-1}^{(i)}+j)} = \tau^{(j)}/(c(z) + \sum_{m=1}^{J_{k|k-1}^{(i)}}\tau^{(m)})$
23. end
24. end
25. $J_k^{(i)} = (l+1)J_{k|k-1}^{(i)},\ \hat{\mathfrak{m}}_k^{(i)} = \sum_{j=1}^{J_k^{(i)}}\eta_k^{(i,j)}$
26. **End**

TABLE III
RB–PHD-FILTER: TRAJECTORY UPDATE

1. **Step 1** (trajectory weight update)
2. **For** $i = 1, \ldots, N$
3. if (26): $\widetilde{w}_k^{(i)} = \lfloor c(z)^{|\mathcal{Z}_k|}\exp^{(\hat{\mathfrak{m}}_k^{(i)} - \hat{\mathfrak{m}}_{k|k-1}^{(i)} - \lambda_c)}\rfloor w_{k-1}^{(i)}$
4. if (27): $j = \{j \in [1, \ldots, J_{k|k-1}^{(i)}] | m^{(i,j)} = \bar{m}\}$ then,
5. $\widetilde{w}_k^{(i)} = \frac{a}{b}w_{k-1}^{(i)}$ where,
6. $a = (1 - P_D)(c(z)^{|\mathcal{Z}_k|}) +$
7. $P_D\eta_{k|k-1}^{(i,j)}(\sum_{z\in\mathcal{Z}_k}(c(z)^{|\mathcal{Z}_k|-1})\mathcal{N}(z; \hat{z}^{(i,j)}, S_k^{(i,j)}))$
8. $b = (c(z)^{|\mathcal{Z}_k|})\eta_k^{(i,j)}$
9. **End**
10. **Step 2** (Resample, if necessary)
11. $\{w_k^{(i)}, X_k^{(i)}, v_k^{(i)}\}_{i=1}^N \sim \{\widetilde{w}_k^{(i)}, \widetilde{X}_k^{(i)}, \widetilde{v}_k^{(i)}\}_{i=1}^N$

TABLE IV
RB–PHD-FILTER: EAP ESTIMATOR

1. **Given** $\{w_k^{(i)}, X_k^{(i)}, v_k^{(i)}\}_{i=1}^N$ and $v_k^{(i)} = \{\eta_k^{(i,j)}, \mu_k^{(i,j)}, P_k^{(i,j)}\}_{j=1}^{J_k^{(i)}}$, a map merging threshold T, set $v_k = \{\eta_k^{(j)}, \mu_k^{(j)}, P_k^{(j)}\}_{j=1}^{J_k} = \{w_k^{(i)}\eta_k^{(1,j)}, \mu_k^{(1,j)}, P_k^{(1,j)}\}_{j=1}^{J_k^{(1)}}$
2. **Step 1** (the expected vehicle trajectory)
3. $\hat{X}_{1:k} = \frac{1}{\bar{w}}\sum_{i=1}^N w_k^{(i)}X_{1:k}^{(i)}$
4. **Step 2** (the expected map PHD, v_k)
5. set i=2, l=0
6. do while$(i <= N)$
7. $l = J_k$
8. for $j = 1, \ldots, J_k^{(i)}$
9. $l = l + 1$
10. $\eta_k^{(l)} = w_k^{(i)}\eta_k^{(i,j)}, \mu_k^{(l)} = \mu_k^{(i,j)}, P_k^{(l)} = P_k^{(i,j)}$
11. end
12. $\mathcal{R} = \{l, \ldots, J_k + J_k^{(i)}\}$
13. do while$(|\mathcal{R}| > 0)$(merge map PHDs)
14. $l = l + 1$
15. $\mathcal{L} = \{r \in \mathcal{R} | (\mu_k^{(j)} - \mu_k^{(r)})^T(P_k^{(j)})^{-1}(\mu_k^{(j)} - \mu_k^{(r)}) \leq T\}$
16. $\eta_k^{(l)} = \sum_{r\in\mathcal{R}}\eta_k^{(r)}$
17. $\mu_k^{(l)} = \frac{1}{\eta_k^{(l)}}\sum_{r\in\mathcal{R}}\eta_k^{(r)}\mu_k^{(r)}$
18. $P_k^{(l)} = \frac{1}{\eta_k^{(l)}}\sum_{r\in\mathcal{R}}\eta_k^{(r)}(P_k^{(j)} + (\mu_k^{(l)} - \mu_k^{(r)})(\mu_k^{(l)} - \mu_k^{(r)})^T)$
19. $J_k = J_k - |\mathcal{L}| + 1,\ \mathcal{R} = \mathcal{R} - \mathcal{L}$
20. end
21. $i = i + 1$
22. end
23. for $j = 1, \ldots, J_k$ (average weights)
24. $\eta_k^{(j)} = \frac{1}{\bar{w}}\eta_k^{(j)}$
25. end
26. **Step 3** (the expected map estimate)
27. $\hat{\mathcal{M}}_k = \emptyset$
28. for $j = 1, \ldots, J_k$
29. if $\eta_k^{(j)} > \tau$
30. $\hat{\mathcal{M}}_k = [\hat{\mathcal{M}}_k\ \mu_k^{(j)}]$
31. end
32. end

approach unifies feature management, DA, and state filtering into a single Bayesian update. While these methods have been used successfully, they generally discard the sensor's detection (P_D) and false alarm (P_{FA}) probabilities and, thus, can be erroneous when subject to large clutter rates and/or measurement noise. Since the proposed approach assumes knowledge of these probabilities, as seen in (23), a modified feature-management routine coined the "feature existence filter" (see Appendix B) which incorporates both P_D and P_{FA}, is used in the benchmark algorithms.

To quantify the map-estimation error, a metric must be adopted that jointly evaluates the error in the feature location *and* number estimates. Current methods typically examine the location estimates of a selected number of features and obtain their MSE using ground truth [5]. As such, vector-based error metrics are applied to feature maps and the error in the estimated *number* of features is neglected. While there are several metrics for finite-set-valued estimation error, that of [13] has been demonstrated to be most suitable [10], [11]. Briefly, the metric optimally assigns each feature estimate to its ground truth through the Hungarian assignment algorithm and evaluates an error distance, while penalizing for under/over estimating the number of features. Based on a second-order Wasserstein construction, if $|\mathcal{M}_k| > |\hat{\mathcal{M}}_k|$, the feature map-estimation error is given by

$$\bar{d}^{(c)}(\hat{\mathcal{M}}_k, \mathcal{M}_k) := \left(\frac{1}{|\mathcal{M}_k|}\left(\min_{j\in\mathrm{perm}(\mathcal{M}_k)}\sum_{i=1}^{|\hat{\mathcal{M}}_k|}d^{(c)}(\hat{m}^i, m^{j(i)})^2 + c^2(|\mathcal{M}_k| - |\hat{\mathcal{M}}_k|)\right)\right)^{1/2} \quad (39)$$

where $d^{(c)}(\hat{m}^i, m^{j(i)}) = \min(c, \|\hat{m}^i - m^{j(i)}\|)$ is the minimum of the cutoff parameter c and the Euclidean distance between the estimated feature location $\hat{m}^i$ and the true feature location

$m^{j(i)}$. If $|\mathcal{M}_k| < |\hat{\mathcal{M}}_k|$, the metric is obtained through $\bar{d}^{(c)}(\mathcal{M}_k, \hat{\mathcal{M}}_k)$. To incorporate oriented features, for instance, other vector distances, such as a Mahalanobis distance, could be used. It is important to note that the error distance of (40) is mathematically consistent, in that the metric satisfies the necessary axioms and enjoys most of the properties of a Euclidean distance. Furthermore, the metric topology is the same as the topology of the underlying space of set-valued maps [13]. In the following sections, this metric along with the estimated trajectory RMSE and graphical comparisons are used to demonstrate the merits of the RB–PHD–SLAM filter.

A. Simulated Dataset

Simulated trials were carried out, due to the ease of generating known ground truth (trajectories and maps) for estimation error evaluation. The parameters for the simulated trials were velocity input standard deviation (std.) of 2 m/s, steering input std. of 5°, range measurement std. of 1 m and bearing measurement std. of 2°, $P_D = 0.95$, $\lambda_c = 20$, using a sensor with 10 m maximum range, and a 360° FoV. The feature existence probability threshold is set at 0.5, and a 95% gate is used throughout. For each SLAM filter, 50 Monte Carlo (MC) trials were carried out in which all methods received identical sequences of control inputs and measurements. The RB-based filters used 50 trajectory particles each, while for MHT-FastSLAM a maximum limit of 2000 particles (number of hypotheses considered prior to resampling) was used.

Fig. 4 shows a sample of the raw input data used in the trials, which is superimposed onto the ground-truth feature map and path. A comparison of the average trajectory-estimation errors for all three filters is then presented in Fig. 5. In terms of the estimated trajectory, the first-order RB–PHD–SLAM algorithm can be seen to outperform the vector-based FastSLAM with robust DA but does not quite achieve the estimation accuracy of JCBB–EKF–SLAM. This is primarily due to the fact that JCBB is very conservative in its choice of measurement–feature associations (jointly compatible constraint) resulting in very few false association pairs influencing the trajectory estimation. However, later results in Figs. 6, 7, and 9 highlight the drawbacks of achieving such impressive localization results.

In terms of the map-estimation component of each SLAM algorithm, Fig. 6 depicts both the true and estimated number of features as the vehicle explores the map, with the proposed RB–PHD–SLAM approach seen to closely track the true number of features in the explored map. Erroneous associations for the MHT-FastSLAM approach result in excessive feature declarations, while the conservative (only including those that are jointly compatible) association decisions of JCBB–EKF–SLAM reduces the number of correct associations. Since vector-based feature-management routines are typically dependant on the DA decisions, this dramatically influences the map-estimation error.

Incorporating the estimation error in both the number and location of features in the map, Fig. 7 plots the map error distance of (39) for each approach. Note that in order to generate this result, the vector-based maps of FastSLAM and

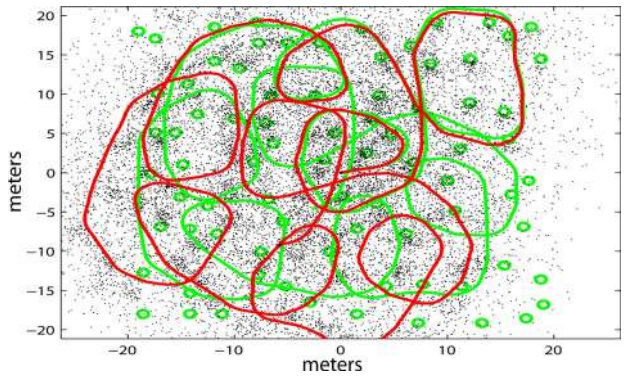

Fig. 4. Simulated environment showing point features (i.e., green circles) and true vehicle trajectory (i.e., green line). A sample measurement history plotted from a sample noisy trajectory (i.e., red line) is also shown (i.e., black points).

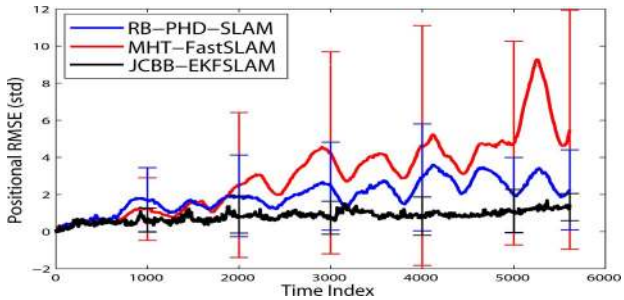

Fig. 5. Mean and std. of the trajectory estimates from each filter over 50 MC runs versus time.

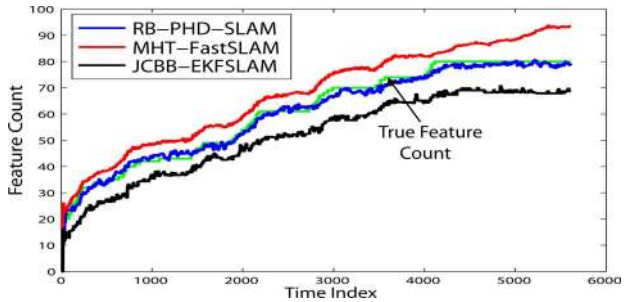

Fig. 6. Average estimated number of features in the map for each filter versus time compared with the ground-truth number of features in the explored map $\mathcal{M}_k$. The feature-number estimate of RB–PHD–SLAM can be seen to closely track that of the ground truth.

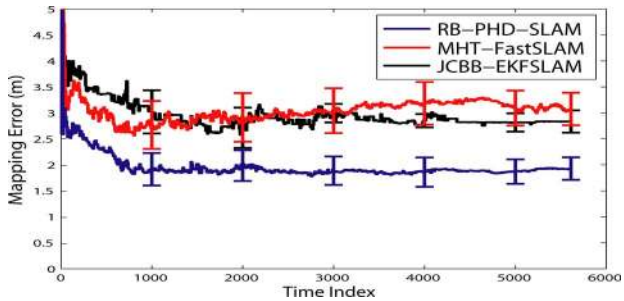

Fig. 7. Comparative plot of the mean and std. of the map-estimation error for each filter versus time. At any given time, for the ideal case, the mapping error from (39) w.r.t. the explored map is zero.

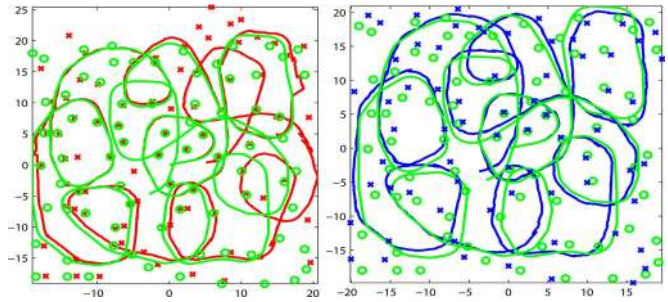

Fig. 8. Comparisons of the posterior SLAM estimates from (left, red) MHT-FastSLAM and the proposed (right, blue) RB–PHD–SLAM. The ground-truth trajectory and map are represented by the green line and circles, respectively. The RB–PHD–SLAM filter demonstrates its robustness and accuracy given high clutter and DA ambiguity.

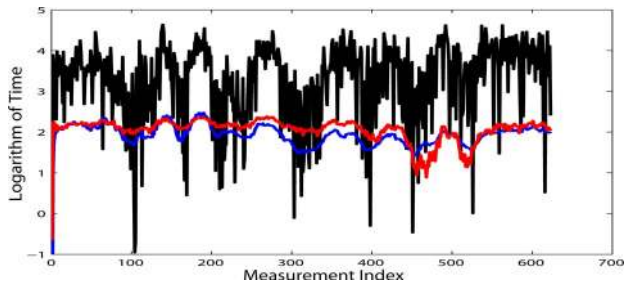

Fig. 9. Comparison of the computation time per measurement update for (blue) RB–PHD–SLAM, (red) MHT-FastSLAM, and (black) JCBB–EKF–SLAM.

JCBB–EKF–SLAM are temporarily "assumed" to be sets. The proposed method can be seen to report the least mapping error due it is robust ability to jointly incorporate uncertainty in feature locations and numbers, while erroneous feature estimates contribute to increased mapping error for the vector-based approaches. A qualitative depiction of the posterior estimates is provided in Fig. 8, demonstrating the usefulness of the RFS–SLAM framework and the proposed RB–PHD–SLAM filter.

B. Complexity and Computation Time

As seen from Section V, the computational complexity of RB–PHD–SLAM is, $\mathcal{O}(\mathfrak{m}_k \mathfrak{z}_k N)$, i.e., linear in the number of features (in the FoV), linear in the number of measurements, and linear in the number of trajectory particles. Furthermore, in contrast to DA-based methods, the proposed approach admits numerous computational enhancements, since the map PHD update of (23) can be segmented, executed in parallel, and subsequently fused for state estimation. This is in contrast with DA-based approaches, which are scalable.

For a single-thread implementation (without the tree-based enhancements [6]), Fig. 9 shows that the computation time is comparable with that of the MHT-FastSLAM algorithm, both of which are less expensive than JCBB–EKF–SLAM as its hypothesis tree grows in the presence of high clutter.

C. Experimental Dataset

This section discusses the filter's performance in a surface-based marine environment, using an X-band radar mounted on a powerboat. In order to maximize the detection of all sea-surface-point features (comprising boats, buoys, etc.), a low detection threshold is required, which subsequently increases the clutter rate. GPS data are available to measure the ground-truth trajectory, while sea charts and data from surrounding vessels' automatic identification systems provide the feature-map ground truth. The test site is off the Southern coast of Singapore, as shown in Fig. 10, where the boat was driven in looping trajectory of 13 km. Adaptive thresholding methods were applied to extract relative-point-measurements from the radar data [36]. The maximum range of the radar, logging at 0.5 Hz, was limited to 1 km. While heading measurements were available via a low-grade onboard single-axis gyroscope, due to the lack of doppler velocity logs, the speed was estimated at eight knots (4.1 m/s).

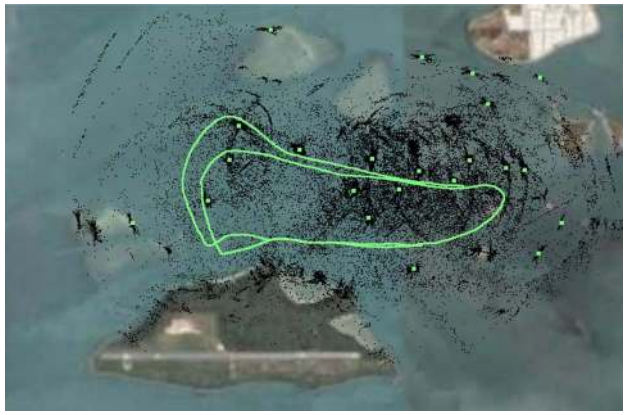

Fig. 10. Overview of the test site (1°13′ N,103°43′ E) showing the (green line) GPS trajectory and (green dots) GPS coordinates of the point-feature map. The (black dots) point-feature-measurement history is also provided.

Fig. 11 compares the posterior SLAM estimates from MHT-FastSLAM and RB–PHD–SLAM, with Fig. 12 comparing the estimated map sizes. The proposed approach can be seen to generate more accurate localization and feature-number estimates; however, it can also be seen that some feature estimates are misplaced in comparison with the ground-truth feature map. The framework is still demonstrated to be useful for high-clutter feature-based SLAM applications.

D. Future Directions

The RFS–SLAM framework proposed in this paper offers numerous extensions and other solutions. For instance, the Poisson assumption of the PHD approach can be relaxed via the cardinalized PHD construct [37] and the multi-Bernoulli recursion [38]. As with the PHD approximation, the trajectory-conditioned measurement likelihood can be calculated exactly for each representation. The proposed RFS framework may also be modified for ML-based approaches [39].

1) RB–CPHD–SLAM: Let the density of the RFS map of (20) be approximated by an iid cluster RFS, which is completely characterized by its cardinality distribution ρ_k and PHD v_k and where $\mathbb{E}[\rho_k] = \int v_k(m)dm$. The trajectory-conditioned map recursion of (15) may then be approximated by a CPHD filter [37], and the trajectory-conditioned-measurement

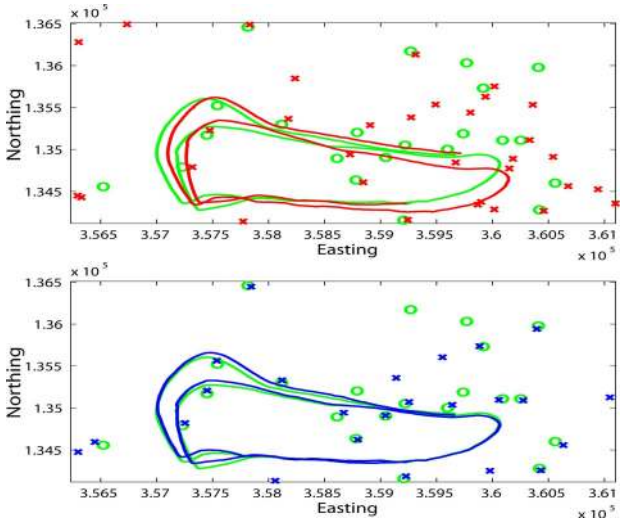

Fig. 11. (Top) Posterior (red) SLAM estimate from MHT-FastSLAM. (Bottom) Posterior (blue) SLAM estimate from RB–PHD–SLAM, in comparison with the (green) ground truth.

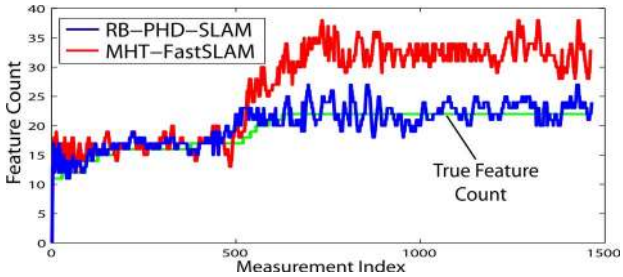

Fig. 12. Comparison of the number of estimated features for each approach. The noisy estimates are likely due to deviations from the Poisson clutter assumption in places.

likelihood of (25) can be evaluated as in [11]. Given that the CPHD filter propagates the *distribution* of the number of features as opposed to just its mean (for the PHD approach of this paper), it is anticipated that the map, and subsequently, the trajectory, estimates from RB–CPHD–SLAM would be remarkably improved in comparison with RB–PHD–SLAM.

2) RB–MeMBer–SLAM: A multi-Bernoulli RFS is simply a set of Bernoulli RFSs, as mentioned previously in Section II-B, and is completely described by the multi-Bernoulli parameter set $\{(\epsilon_k^{(i)}, \pi_k^{(i)})\}_{i=1}^{\mathrm{m}_k}$. As with RB–CPHD–SLAM, if the RFS map density of (15) is approximated by a multi-Bernoulli RFS, the trajectory-conditioned map recursion of (15) may be approximated by a MeMBer filter [38], and again, the trajectory-conditioned-measurement likelihood of (25) can be evaluated, as in [11].

Differing from RB–PHD–SLAM and RB-CPHD–SLAM, RB–MeMBer–SLAM propagates a set of features and their corresponding existence probabilities. Using a Bernoulli RFS to represent each feature allows for the joint encapsulation of its existence probability and location in a single pdf, thus enhancing existing approaches in SLAM, which typically model the existence probability and location as separate independent entities [5], [6]. It is expected that RB–MeMBer–SLAM would perform well in the presence of highly nonlinear process and/or measurement models.

3) ML–RFS–SLAM: In contrast to the aforementioned RBPF solutions, the proposed RFS–SLAM framework can also be adapted to the popular ML approaches, which formulate SLAM as a nonlinear stochastic optimization problem [39], [40]. Recently, methods to estimate the parameters of the measurement likelihood from the PHD filter using SMC have been proposed [41]. Assuming a finite-set measurement and state, the gradient of the likelihood function was estimated and used to determine the ML estimate of the unknown measurement parameters such as the clutter rate. Thus, the RFS–SLAM framework can also admit ML-type vehicle-trajectory estimation, such as in [40]. By formulating a suitable likelihood function and estimating the feature map using the proposed PHD/CPHD/MeMBer methods, gradients could be evaluated to extract the ML vehicle trajectory.

VII. Conclusion

This paper establishes that, from a fundamental estimation viewpoint, a feature-based map is a finite set and subsequently presented a Bayesian-filtering formulation, as well as a tractable solution for the feature-based SLAM problem. The filter jointly propagates and estimates the vehicle trajectory, the number of features in the map, as well as their individual locations in the presence of DA uncertainty and clutter. The key to the approach is to adopt the natural finite-set representation of the map and to use the tools of finite-set statistics to cast the problem into the Bayesian paradigm. It is shown that this Bayesian formulation admits a number of optimal Bayes estimators for SLAM. The finite-set representation of the map admits the notion of expected map in the form of a PHD or intensity function. The PHD construct can also be interpreted in terms of occupancy maps. An RB implementation of the filter was proposed, in which the PHD of the map was propagated using a GM PHD filter, and a particle filter propagated the vehicle trajectory density.

Analysis was carried out both in a simulated environment through MC trials and an outdoor SLAM experimental dataset based on an X-band marine radar sensor. Results demonstrated the robustness of the proposed filter, particulary in the presence of large DA uncertainty and clutter, illustrating the merits of adopting an RFS approach to SLAM. Furthermore, the framework admits numerous avenues of future research into ML approaches or enhancements via the CPHD and MeMBer filters, which are expected to improve the performance and increase robustness to clutter, DA difficulty and highly nonlinear process/measurement models.

Appendix A

Derivation of $g_k(\mathcal{Z}_k|\mathcal{Z}_{0:k-1}, X_{0:k})$ for the Rao–Blackwellized–Probability Hypothesis Density–Simultaneous Localization and Mapping Filter

Recalling (15), we have

$$p_k(\mathcal{M}_k|X_{0:k}) = \frac{g_k(\mathcal{Z}_k|\mathcal{M}_k, X_k)p_{k|k-1}(\mathcal{M}_k|X_{0:k})}{g_k(\mathcal{Z}_k|\mathcal{Z}_{0:k-1}, X_{0:k})}$$

and the Poisson RFS approximations

$$p_{k|k-1}(\mathcal{M}_k|X_{0:k}) \approx \frac{\prod_{m\in\mathcal{M}_k} v_{k|k-1}(m|X_{0:k})}{\exp\left(\int v_{k|k-1}(m|X_{0:k})dm\right)}$$

$$p_k(\mathcal{M}_k|X_{0:k}) \approx \frac{\prod_{m\in\mathcal{M}_k} v_k(m|X_{0:k})}{\exp\left(\int v_k(m|X_{0:k})dm\right)}.$$

Rearranging and assigning $\mathcal{M}_k = \emptyset$ gives

$$\begin{aligned} g_k(\mathcal{Z}_k|\mathcal{Z}_{0:k-1}, X_{0:k}) &= g_k(\mathcal{Z}_k|\emptyset, X_k) \\ &\quad \times \frac{\prod_{m\in\mathcal{M}_k} v_{k|k-1}(m|X_{0:k})}{\prod_{m\in\mathcal{M}_k} v_k(m|X_{0:k})} \\ &\quad \times \frac{\exp\left(\int v_k(m|X_{0:k})dm\right)}{\exp\left(\int v_{k|k-1}(m|X_{0:k})dm\right)} \end{aligned}$$

Since $\mathcal{M}_k = \emptyset$, the empty-set-measurement likelihood is that of the clutter RFS (Poisson)

$$g_k(\mathcal{Z}_k|\emptyset, X_k) = \frac{\prod_{z\in\mathcal{Z}_k} c_k(z|X_k)}{\exp(\int c_k(z|X_k)dz)}.$$

Both $\prod_{m\in\mathcal{M}_k} v_{k|k-1}(m|X_{0:k})$ and $\prod_{m\in\mathcal{M}_k} v_k(m|X_{0:k})$ are empty, thereby implying that their product is 1, $\hat{\mathfrak{m}}_{k|k-1} = \int v_{k|k-1}(m|X_{0:k})dm$, and $\hat{\mathfrak{m}}_k = \int v_k(m|X_{0:k})dm$, giving

$$\begin{aligned} g_k(\mathcal{Z}_k|\mathcal{Z}_{0:k-1}, X_{0:k}) &= \prod_{z\in\mathcal{Z}_k} c_k(z|X_k) \\ &\quad \times \exp\left(\hat{\mathfrak{m}}_k - \hat{\mathfrak{m}}_{k|k-1} - \int c_k(z|X_k)dz\right). \end{aligned}$$

Note that while, for the empty map choice, the likelihood $g_k(\mathcal{Z}_k|\mathcal{Z}_{0:k-1}, X_{0:k})$ does not contain a measurement likelihood term $g_k(\mathcal{Z}_k|\mathcal{M}_k, X_k)$, the history of measurements and trajectories are incorporated into the predicted and updated intensity terms, whose integrals appear as the terms $\hat{\mathfrak{m}}_{k|k-1}$ and $\hat{\mathfrak{m}}_k$, respectively.

APPENDIX B
FASTSLAM FEATURE MANAGEMENT

This Appendix outlines the feature-management routine developed for the benchmark filters, incorporating the detection and false-alarm probabilities for a fair comparison with the RB–PHD–SLAM filter. As with standard approaches [5], tentative new features are declared for unassociated measurements. The "existence probability" of each feature $P^{(j)}_{E,k}$, given a 95% confidence gate and prior existence probability of $P^{(j)}_{E,k-1}$, then evolves through a binary Bayes filter according to the routine of Table V. This *ad hoc* but effective routine enhances the robustness of standard SLAM feature management when exposed to high clutter rates. Thus, both the benchmark and proposed approach receive the same information for each filter loop.

TABLE V
FEATURE EXISTENCE FILTER

Step 1: (Obtain association details within FoV)

$$\bar{J} = \{j \in M_k | m^j \in \text{FoV } \&\ m^j \text{ not associated.}\}$$

$$J = \{j \in M_k | m^j \in \text{FoV } \&\ m^j \text{ associated.}\}$$

Step 2: (Calculate hit, miss and association probabilities)

$$P^{(\bar{J})}_{miss} = (1 - P_D) \times P^{(\bar{J})}_{E,k-1} + P_D \times 0.05 \times P^{(\bar{J})}_{E,k-1}$$

$$P^{(J)}_{hit} = P_D \times P^{(J)}_{assoc} P^{(J)}_{E,k-1}$$

$$P^{(J)}_{assoc} = \frac{1}{2\pi}|S_k|^{-1/2} \exp(-\frac{1}{2}\upsilon S_k^{-1}\upsilon^T)$$

Step 3: (Update Existence probabilities)

$$P^{(\bar{J})}_{E,k} = \frac{P^{(\bar{J})}_{miss}}{P^{(\bar{J})}_{miss} + (1 - P_{FA})(1 - P^{(\bar{J})}_{E,k-1})}$$

$$P^{(J)}_{E,k} = \frac{P^{(J)}_{hit}}{P^{(J)}_{hit} + P_{FA}(1 - P^{(J)}_{E,k-1})}$$

ACKNOWLEDGMENT

The authors thank the reviewers for their valuable comments.

REFERENCES

[1] R. Smith, M. Self, and P. Cheeseman, "Estimating uncertain spatial relationships in robotics," in *Autonomous Robot Vehicles*, New York: Springer, 1990, pp. 167–193.
[2] S. Thrun, "Particle filter in robotics," presented at Uncertainty AI, Edmonton, AB, Canada, 2002.
[3] D. Makarsov and H. F. Durrant-Whyte, "Mobile vehicle navigation in unknown environments: A multiple hypothesis approach," *Inst. Electr. Eng. Proc. Contr. Theory Appl.*, vol. 142, pp. 385–400, Jul. 1995.
[4] J. Guivant, E. Nebot, and S. Baiker, "Autonomous navigation and map building using laser range sensors in outdoor applications," *J. Robot. Syst.*, vol. 17, no. 10, pp. 565–583, Oct. 2000.
[5] G. Dissanayake, P. Newman, H. F. Durrant-Whyte, S. Clark, and M. Csorba, "A solution to the simultaneous localization and map building (SLAM) problem," *IEEE Trans. Robot. Autom.*, vol. 17, no. 3, pp. 229–241, Jun. 2001.
[6] M. Montemerlo, S. Thrun, and B. Siciliano, *FastSLAM: A Scalable Method for the Simultaneous Localization and Mapping Problem in Robotics*. New York: Springer-Verlag, 2007.
[7] H. F. Durrant-Whyte and T. Bailey, "Simultaneous localization and mapping: Part I," *IEEE Robot. Autom. Mag.*, vol. 13, no. 2, pp. 99–110, Jun. 2006.
[8] J. Niera and J. D. Tardos, "Data association in stochastic mapping using the joint compatibility test," *IEEE Trans. Robot. Autom.*, vol. 17, no. 6, pp. 890–897, Dec. 2001.
[9] J. Mullane, B. N. Vo, M. Adams, and W. S. Wijesoma, "A random set formulation for Bayesian SLAM," in *Proc. IEEE/RSJ Int. Conf. Intell. Robots Syst.*, Sep. 2008, pp. 1043–1049.
[10] J. Mullane, B. N. Vo, M. Adams, and W. S. Wijesoma, "A random set approach to SLAM," in *Proc. IEEE Int. Conf. Robot. Autom. Workshop Vis. Mapp. Navigat. Outdoor Environ.*, May 2009, pp. 1–7.
[11] J. Mullane, B. N. Vo, and M. Adams, "Rao–Blackwellised PHD SLAM," in *Proc. IEEE Int. Conf. Robot. Autom.*, May 2010, pp. 5410–5416.
[12] J. R. Hoffman and R. Mahler, "Multi-target miss distance via optimal assignment," *IEEE Trans. Syst., Man Cybern.*, vol. 34, no. 3, pp. 327–336, May 2004.
[13] D. Schuhmacher, B. T. Vo, and B. N. Vo, "A consistent metric for performance evaluation of multi-object filters," *IEEE Trans. Signal Process.*, vol. 86, no. 8, pp. 3447–3457, 2008.
[14] G. Grisetti, C. Stachniss, and W. Burgard, "Improved techniques for grid mapping with Rao–Blackwellized particle filters," *IEEE Trans. Robot.*, vol. 23, no. 1, pp. 34–45, Feb. 2007.

[15] Y. Rachlin, J. M. Dolan, and P. Khosla, "Efficient mapping through exploitation of spatial dependencies," in *Proc. IEEE/RSJ Int. Conf. Intell. Robots Syst.*, Edmonton, AB, Canada, Aug. 2005, pp. 3117–3122.
[16] R. Mahler, "Multi-target Bayes filtering via first-order multi-target moments," *IEEE Trans. AES*, vol. 4, no. 39, pp. 1152–1178, Oct. 2003.
[17] R. Mahler, *Statistical Multisource Multitarget Information Fusion*. Norwood, MA: Artech, 2007.
[18] B. N. Vo, S. Singh, and A. Doucet, "Sequential monte carlo methods for multi-target filtering with random finite sets," *IEEE Trans. Aerosp. Electron. Syst.*, vol. 41, no. 4, pp. 1224–1245, Oct. 2005.
[19] M. Tobias and A. Lanterman, "A probability hypothesis density based multitarget tracking with multiple bistatic range and doppler observations," *Proc. Inst. Electr. Eng. Radar Sonar Navigat.*, vol. 152, no. 3, pp. 195–205, 2005.
[20] T. Wood. (Feb. 2010). Random finite set theory for tracking [Online]. Available: http://people.maths.ox.ac.uk/ woodtm/rfs_overview.pdf.
[21] B. T. Vo, "Random finite sets in multi-object filtering," Ph.D. dissertation, Univ. Western Australia, Perth, W.A., Australia, 2008.
[22] R. Mahler, "Implementation and application of PHD/CPHD filters," presented at the Int. Conf. Inf. Fusion, Seattle, WA, 2009.
[23] S. Kay, *Fundamentals of Statistical Signal Processing, Vol I—Estimation Theory*. Englewood Cliffs, NJ: Prentice-Hall, 1998.
[24] C. Roberts, *The Bayesian Choice: From Decision-Theoretic Foundations to Computational Implementation*. New York: Springer-Verlag, 2001.
[25] R. Murphy, "Bayesian map learning in dynamic environments," in *Proc. Conf. Neural Inf. Process. Syst.*, 1999, pp. 1015–1021.
[26] P. D. Moral and J. Jacod, *The Monte-Carlo Method for Filtering With Discrete Time Observations. Central Limit Theorems.* Providence, RI: Fields Inst. Commun. Amer. Math. Soc., 2002.
[27] D. Crisan and A. Doucet, "A survey of convergence results on particle filtering methods for practitioners," *IEEE Trans. Signal Process.*, vol. 50, no. 3, pp. 736–746, Mar. 2002.
[28] D. J. Daley and D. Vere-Jones, *An Introduction to the Theory of Point Processes*. New York: Springer-Verlag, 2002.
[29] D. Stoyan, W. S. Kendall, and J. Mecke, *Stochastic Geometry and Its Applications*, 2nd ed. New York: Wiley, 1995.
[30] A. Brooks and T. Bailey, "Hybrid SLAM: Combining FastSLAM and EKF-SLAM for reliable mapping," presented at the 8th Int. Workshop Algorithmic Found. Robot., Guanajuato, Mexico, Dec. 2008.
[31] O. Erdinc, P. Willett, and Y. Bar-Shalom, "The bin-occupancy filter and its connection to the PHD filters," *IEEE Trans. Signal Process.*, vol. 57, no. 11, pp. 4232–4246, Nov. 2009.
[32] B. Kaylan, K. W. Lee, and W. S. Wijesoma, "FISST-SLAM: Finite set statistical approach to simultaneous localization and mapping," *Int. J. Robot. Res.*, vol. 29, no. 10, pp. 1251–1262, Sep. 2010. Published online before print Oct. 1, 2009, doi: 10.1177/0278364909349948.
[33] H. F. Durrant-Whyte, S. Majumder, M. de Battista, and S. Scheding, "A Bayesian algorithm for simultaneous localisation and map building," presented at the 10th Int. Symp. Robot. Res., Lorne, Vic., Australia, 2001.
[34] B. N. Vo and W. K. Ma, "The Gaussian mixture probability hypothesis density filter," *IEEE Trans. Signal Process.*, vol. 54, no. 11, pp. 4091–4104, Nov. 2006.
[35] J. Nieto, J. Guivant, E. Nebot, and S. Thrun, "Real time data association for FastSLAM," in *Proc. IEEE Int. Conf. Robot. Autom.*, Sep. 2003, vol. 1, pp. 412–418.
[36] J. Mullane, S. Keller, A. Rao, M. Adams, A. Yeo, F. Hover, and N. Patrikalakis, "X-band radar based SLAM in Singapores off-shore environment," in *Proc. IEEE 11th IEEE ICARCV*, Singapore, Dec. 2010.
[37] B. T. Vo, B. N. Vo, and A. Cantoni, "Analytic implementations of the cardinalized probability hypothesis density filter," *IEEE Trans. Signal Process.*, vol. 55, no. 7, pp. 3553–3567, Jul. 2007.
[38] B. T. Vo, B. N. Vo, and A. Cantoni, "The cardinality balanced multi-target multi-bernoulli and its implementations," *IEEE Trans. Signal Process.*, vol. 57, no. 2, pp. 409–423, Feb. 2009.
[39] M. Kaess, A. Ranganathan, and F. Dellaert, "iSAM: Incremental smoothing and mapping," *IEEE Trans. Robot.*, vol. 24, no. 6, pp. 1365–1378, Dec. 2008.
[40] E. Olson, J. Leonard, and S. Teller, "Fast iterative optimization of pose graphs with poor initial estimates," in *Proc. IEEE Int. Conf. Robot. Autom.*, May 2006, pp. 2262–2269.
[41] S. S. Singh, N. Whiteley, and S. Godsill, "An approximate likelihood method for estimating the static parameters in multi-target tracking models," Cambridge, U.K., Tech. Rep., 2009.

John Mullane received the B.E.E degree (with first-class honors) in electrical and electronic engineering from the University College Cork, Ireland, in 2002 and the Ph.D. degree from Nanyang Technological University (NTU), Singapore, in 2009.

He is currently a Postdoctoral Research Fellow with the Department of Electrical and Electronic Engineering, NTU, as a part of the Singapore–Massachusetts Institute of Technology Alliance for Research and Technology. His current research interests include radar signal processing, probabilistic mapping, and stochastic mobile robotics.

Ba-Ngu Vo received the Bachelor degrees jointly in science and electrical engineering (with first-class honors) from the University of Western Australia, Crawley , W.A., Australia, in 1994, and the Ph.D. degree from the Curtin University of Technology, Perth, W.A., in 1997.

He held various research positions before joining the Department of Electrical and Electronic Engineering, University of Melbourne, Melbourne, Australia, in 2000. He is currently a Winthrop Professor and the Chair of signal processing with the School of Electrical Electronic and Computer Engineering, University of Western Australia. His current research interests include signal processing, systems theory, and stochastic geometry with emphasis on target tracking, robotics, and computer vision.

Dr. Vo is a recipient of the Australian Research Council's inaugural Future Fellowship.

Martin D. Adams received the degree in engineering science and the D.Phil. degree from the University of Oxford, Oxford, U.K., in 1988 and 1992, respectively.

He was with the Swiss Federal Institute of Technology, Lausanne, Switzerland, and the European Semiconductor Equipment Center before joining Nanyang Technological University, Singapore. In 2010, he joined the University of Chile, Santiago, Chile, where he currently serves as a Professor with the Department of Electrical Engineering. He is also a member of the Advanced Mining Technology Center. His current research interests include stochastic estimation and signal processing with applications in autonomous robot navigation, sensing, and control.

Ba-Tuong Vo received the B.Sc. degree in applied mathematics and the B.E. degree in electrical and electronic engineering (with first-class honors) in 2004 and the Ph.D. degree in engineering (with distinction) in 2008, all from the University of Western Australia, Crawley, W.A., Australia.

He is currently an Assistant Professor and the Australian Postdoctoral Fellow with the School of Electrical, Electronic and Computer Engineering, University of Western Australia. His current research interests include point-process theory, filtering and estimation, and multiple-object filtering.